Stem Cell Research & Therapy

RESEARCH

Open Access

Cathepsin K inhibition promotes efficient differentiation of human embryonic stem cells to mature cardiomyocytes by mediating glucolipid metabolism and cellular energy homeostasis

Ying Wang[1], Yang Cui[1], Xiaoyu Liu[1], Shengxian Liang[1], Li Zhong[2] and Rui Guo[1,3*]

Abstract

Background and aim Generation of functional cardiomyocytes from human pluripotent stem cells (hPSCs) offers promising applications for cardiac regenerative medicine. Proper control of pluripotency and differentiation is vital for generating high-quality cardiomyocytes and repairing damaged myocardium. Cathepsin K, a lysosomal cysteine protease, is a potential target for cardiovascular disease treatment; however, its role in cardiomyocyte differentiation and regeneration is unclear. This study aims to investigate the effects and mechanisms of cathepsin K inhibition on the differentiation of human embryonic stem cell-induced cardiomyocytes (hESC-CMs) and myocardial generation.

Methods We cultured H9-hESCs in CDM3 medium to induce myocardial differentiation, adding cathepsin K inhibitor II (1 μM) on days 2, 5 and 8, respectively. Cells were observed and collected 48 h after each treatment. The morphology and contractile clusters of H9-hESCs were tracked with microscopy and video recording. Pluripotency and cardiac markers were assessed at each stage of differentiation. We also examined glucose and lipid metabolism, mitochondrion-related markers, apoptosis and autophagy.

Results CDM3 medium effectively differentiated high-density H9-hESCs into mature, spontaneously contracting cardiomyocytes. Cathepsin K inhibition accelerates the differentiation of H9-hESCs into cardiac mesoderm and cardiac precursor cells (CPCs) by reducing apoptosis, decreasing glycolysis and fatty acid metabolism at the early and middle stages, and subsequently facilitate the development and differentiation of cardiomyocytes by enhancing glucolipid metabolism and oxidative phosphorylation at the late stage. Meanwhile, cathepsin K inhibition enhanced mitochondrial function and lysosome-related gene transcription during the differentiation process.

Conclusion Our study highlights the potential of cathepsin K inhibition for renewable cardiomyocytes and suggests exploring metabolic pathways and signaling to improve cardiac regeneration and organoid development.

Keywords Human embryonic stem cell, Cathepsin K, Cardiomyocyte differentiation, Energy metabolism, Mitochondrion, Lysosome, Autophagy

*Correspondence:
Rui Guo
rguo@hbu.edu.cn
Full list of author information is available at the end of the article

Graphical abstract

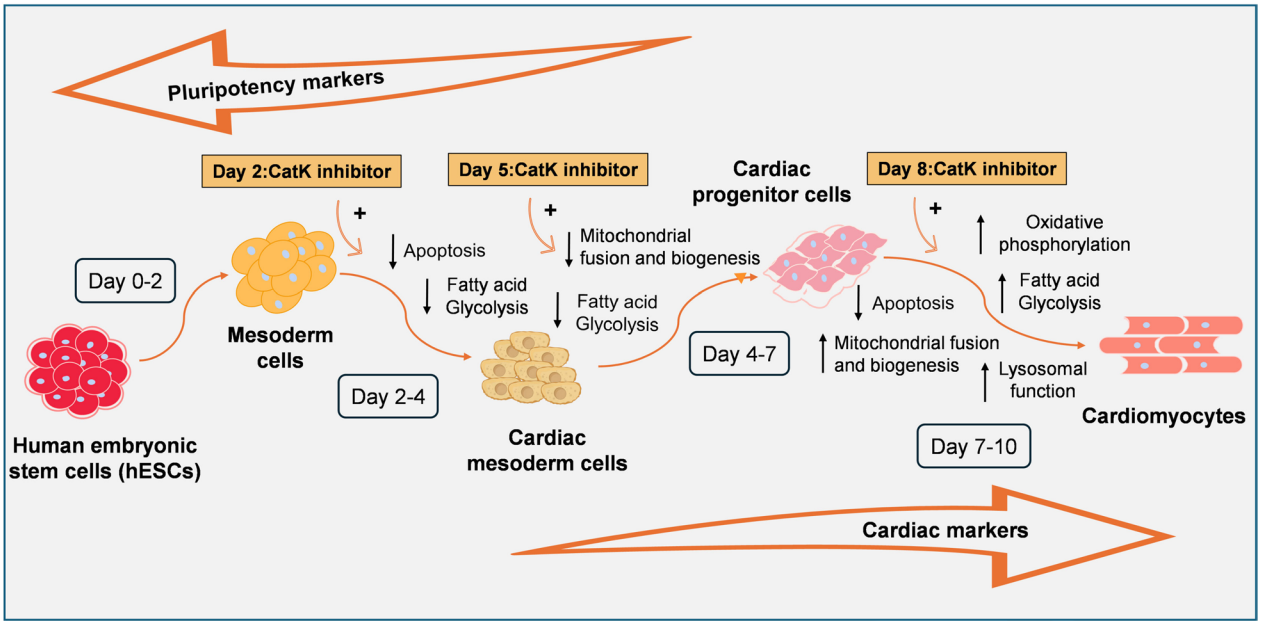

Background

Cardiovascular disease (CVD) remains the leading cause of global morbidity and mortality due to a combination of aging, hereditary and environmental factors. By 2030, the aging population in the world is expected to reach 20%, and the prevalence of CVD will rise exponentially [1]. Despite improvements in healthcare that have increased the number of CVD survivors, the irreparable damage to the heart tissue and the limited capacity for myocardial regeneration has a significant negative impact on the survivors' quality of life. Therefore, it is imperative to explore medications and therapeutic approaches with clinical applicability [2]. Production of functional cardiomyocytes from human pluripotent stem cells (hPSCs) provide enormous potentiality and applications for cardiac regenerative medicine, such as the development of cardiac organoids and cell transplantation for tissue repair. Accordingly, it is crucial to optimize culture conditions and make proper regulation of cellular pluripotency and differentiation to generate high quality of cardiomyocytes for the repair of damaged myocardium [3–5].

Stem cell therapy for cardiac repair has drawn wide attention in biomedical field due to its capability of immune regulation, anti-inflammatory properties, promoting the expression of paracrine factors, homing and regeneration ability [6, 7]. The ultimate goal of repairing cardiac damage in the process of stem cell therapy is to improve cardiac function and restore myocardial vitality by the regeneration of working cardiomyocytes with mature electrophysiological characteristics and advanced contractile properties [8, 9]. Human embryonic stem cells (hESCs) and human induced pluripotent stem cells (hiPSCs) are two types of hPSCs that possess the unique capacity to differentiate into various cell types in the human body. This remarkable characteristic makes them highly valuable for both experimental and clinical applications [10–12]. Because of the possible ethical issues, researchers have successfully established and derived hESCs by a process called somatic-cell nuclear transfer [13]. The cells can be now produced more reliably and quickly. David Cyranoski also emphasized the clinical prospect of hESCs in *Nature*, and indicated that hESCs are much safer than hiPSCs, although the latter offer greater potential for conducting disease-in-a-dish studies [12]. Zhang's team also emphsized that ESC-derived cardiomyocytes perform better than iPSC-derived cardiomyocytes (iPSC-CM) [14]. Nevertheless, both hESCs and hiPSCs have exhibited immense potential for cell transplantation, cell therapy and organogenesis.

The differentiation process of cardiomyocytes induced by hPSCs involves several key signaling pathways and growth factors including bone morphogenetic proteins (BMPs), Wnt signaling, Notch signaling, activin A, and fibroblast growth factor, which are essential for the development of early cardiac mesodermal cells. These signals and factors are highly conserved across various

species and are able to initiate specific combinations of heart-specific transcription factors [15–17]. These highly conserved gene regulatory networks control the initial differentiation, proliferation and maturation hESC-CMs through a variety of complex interactions. The maturation process of hESC-CMs begins with the precursor cells, and eventually forms functional cardiomyocytes [18]. Currently, a highly effective and stable strategy for differentiation involves activating the Wnt signaling pathway with small molecules to promote hESC differentiation into the mesoderm. An intact mitochondrial fusion is essential for transcriptional factors, such as TGF-β/BMP, serum response factor, GATA4, and MEF2, which are linked to increased Ca^{2+}-dependent calcineurin activity and Notch1 signaling, driving mesodermal cell differentiation into cardiac precursor cells and cardiomyocytes [19]. In addition, endogenous glucocorticoid cortisol, IGF1, insulin, thyroid hormone tri-iodothyronine, and dexamethasone can also promote cardiac maturation in developing hearts and hiPSC-CMs through receptor interactions, and are commonly included in maturation media [20]. Although there are various methods for the induction of hESCs to cardiomyocytes, current bottlenecks and urgent challenges are still needed [3, 21, 22]. Thus, to find an alternative strategy to enhance the differentiation and quality of cardiomyocytes from PSCs, and promote myocardial repair after myocardial injury is extremely important.

Both hESC-CMs and iPSC-CMs may exhibit immature structural phenotypes and aberrant electrophysiological characteristics resembling fetal-like cardiomyocytes. The metabolism of mature PSC-CMs resembles that of a newborn on the first day of life [23]. Evidence has suggested that energy metabolism, such as glycolysis, mitochondrial oxidative phosphorylation and fatty acid β-oxidation exhibit vital influence on cardiomyocyte proliferation, differentiation, and postnatal maturation. The alterations in energy substrate metabolism can affect the expression of stemness factors during the process of cardiomyocyte differentiation as the heart matures [24]. Garbern et al. reviewed that mitochondria play a crucial role in driving the maturation of cardiomyocytes by sensing nutrient signals, regulating respiratory capacity and modulating reactive oxygen species (ROS) production. They provide ATP necessary for differentiation, initiate transcriptional and epigenetic modifications that guide the process of cardiomyocyte maturation [25]. Indeed, mitochondria in stem cells are initially immature to protect against ROS-induced cytotoxicity. Upon differentiation, mitochondrial content increases, with morphological changes like fusion and enlargement, along with a significant rise in mitochondrial activity [26]. As embryos mature, mitochondria diversify to adapt to developmental energy demands. After the perinatal period, fetal metabolism transitions from glycolysis to the more efficient fatty acid β-oxidation [27]. Similarly, PSC-CMs show less efficient calcium handling, fewer and underdeveloped mitochondria, and use glucose as primary energy source rather than using fatty acid in maturated/adult cardiomyocytes [7, 28]. In addition, iPSC-CMs were reported to display morphological disarray, compromised contractile capacity, and altered glycolytic metabolism [8, 15]. In addition, lysosomes are also considered indispensable for regulating the reprogramming of stem cell identity transitions and metabolic networks. Its biogenesis mechanism holds significant implications for cell maintenance and renewal [29]. As a lysosomal degradation pathway, autophagy is essential for myocardial terminal differentiation by protecting cells from nutrient shortages [30, 31].

Several types of cathepsins have been reported to be involved in embryonic development and cell differentiation by regulating different intracellular catabolism [32]. Cathepsin L has been shown to regulate the developmentally-controlled cleavage of H3 during ESC differentiation [33]. Cathepsin A led to reduced pluripotency, impaired proliferation due to cell cycle arrest, and decreased differentiation potential and teratoma formation in mouse ESCs [34]. Cathepsin K, as one of the most potent lysosomal cysteine proteases, is expressed in different types of tissues and stem/progenitor cells, and functions range from bone homeostasis, protein turnover, adipogenesis, hormone regulation and modulation of growth factors [35, 36]. Inappropriate cathepsin K elevation or secretion was shown to be associated with varieties of metabolic disorders such as obesity, diabetic cardiomyopathy, atherosclerosis, and tumor metastasis. On the contrary, inhibition of cathepsin K exhibited protective effect against diabetes, aging, cardiovascular defects and cancer by regulating energy metabolism, calcium handling, inflammation, NF-kB signaling, Akt/IGF-1 signaling or/and mitochondria-mediated apoptotic pathways [37–44]. In addition, cathepsin K has been displayed consistent collagenase activity under neutral conditions, suggesting its stability and adaptability [45, 46]. Cathepsin K was also reported to be associated to periosteal stem cell differentiation and function [47]. Its deficiency enhances alveolar bone regeneration by stimulating the proliferation and differentiation of jaw bone marrow mesenchymal stem cells through the glycolysis pathway [48]. However, the role of cathepsin K inhibitor in the differentiation of hESCs to cardiomyocytes is still poorly understood.

Based on the potential and unique biological functions of cathepsin K in the regulation of cardiovascular homeostasis, this study aims to investigate the effects and underlying mechanisms of cathepsin K inhibition on the differentiation of hESC-CMs and myocardial

regeneration. Therefore, we investigated the effects of cathepsin K inhibitor II on the morphology and the spontaneous contractile clusters of H9-hESCs by using microscopy and video recorder during the whole differentiation period. The pluripotency of H9-hESCs and the expression of cardiac markers were detected at each stage of induction. Key metabolic parameters and markers associated with glucose and lipid metabolism, mitochondrial fusion and biogenesis, apoptosis and autophagy were examined. Gaining insights into the metabolic mechanisms governing stem cell homeostasis and differentiation could offer new perspectives for tissue regeneration and disease management.

Result

Myocardial differentiation and growth characteristics of H9-hESCs

Morphological changes serve as prominent indicators of the health status of human pluripotent stem cells (hPSCs) throughout the cardiomyocyte differentiation process. Consequently, we meticulously documented the transition from H9-hESCs to differentiated pulsating cardiomyocyte masses. In their undifferentiated state, the original H9-hESCs gradually aggregated, with clusters of dozens to hundreds of cells rapidly proliferated. When the colony density reached around 80%, individual cells were resuspended to initiate differentiation (Fig. 1A). This process involved the application of small molecules and CDM3-based methods to induce the transformation of H9-hESCs into cardiomyocytes (Fig. 1B). Within a span of ten days following the initiation of differentiation, the cells progressed through three distinct stages including mesoderm and cardiac mesoderm formation, development into cardiac precursor cells (CPCs), and ultimately, maturation into cardiomyocytes. H9-hESC-CMs showed obvious cell morphological changes throughout continuous differentiation (Fig. 1C). Starting from the seventh day of differentiation, local clusters of spontaneous myocardial contractions gradually appeared within the multicellular environment of the culture dish. Simultaneously, peripheral cardiomyocytes underwent successive stages of differentiation and maturation, leading to the development of functional contraction clusters distinguished by their consistent rhythmic beating. By the tenth day of differentiation, the myocardial contractile mass was essentially established, visibly contracting and beating akin to a heart when observed under the microscope (Fig. 1C, Video S1). Occasionally, we also observed several localized contractile cell masses as shown in Fig. 1D and Video S2. In comparison to normal AC16 cardiomyocytes, H9-hESC-CMs from day 10 exhibited similar size, a fibrocyte-liked appearance and adherence to the substrate of the culture flask (Fig. S1A).

Screening and enrichment of differentially expressed genes during hESC-CMs differentiation under Wnt regulation

To investigate the impact of Wnt signaling on myocardial differentiation of hESCs, we conducted bioinformatic analysis of differentially expressed genes (DEGs) using the dataset GSE67154, comparing the FBW and FB groups across time points on days 2, 4, 6, and 8. Based on p-value < 0.05 and $|\log2\ FC| > 1$, 1,917 upregulated and 2,151 downregulated DEGs were screened in the GSE67154 dataset. DAVID functional enrichment analysis identified 188 significant biological processes (BP) during the differentiation of hESCs (Excel S1). The most significantly enriched functional pathways included the hypoxia response, the canonical Wnt-signaling pathway, and its negative regulation (Fig. 2A). The cellular component (CC) enrichment analysis identified 61 core terms (Excel S2), which were predominantly associated with the cytosol, cytoplasm, glutamatergic synapse, membranes, and extracellular exosomes among other components (Fig. 2B). In addition, the DEGs exhibited 61 molecular functions (MF) (Excel S3), mostly related to protein binding and gene recognition (Fig. 2C). KEGG pathway analysis identified 38 signaling pathways involved in the differentiation of hESC-CMs (Supplementary Excel 4). The most significantly enriched pathways included glycolysis/gluconeogenesis, Wnt signaling, cancer signaling, fructose and mannose metabolism, as well as glutamate synapse and metabolic pathways. Moreover, genes and pathways related to fatty acid metabolism and mitochondrial energy production were also identified and found to be significantly enriched (Excel S4, Fig. 2D).

Cathepsin K inhibitor facilitates the differentiation of H9-hESCs into cardiomyocytes

To evaluate the mechanism of cathepsin K inhibitor in regulating cardiomyocyte formation during different stages of H9-hESCs differentiation, the CDM3 culture model was used to induce cardiomyocyte maturation (Fig. 1B). Cathepsin K inhibitor II was added to the cells on day 2, day 5 and day 8, respectively. On the seventh day of differentiation, aggregates began forming with abundant spontaneously contracting clusters of cardiomyocytes in the cathepsin K inhibitor II treatment group. By the nineth day, a layer of cells exhibited consistent rhythmic contractions indicative of cardiac pulsation (Fig. 3A, Video S3). On days 4 and 10, we observed no notable changes in cell morphology and contraction between control and inhibitor groups (Fig. S1B, Video S1 and Video S4). However, on day 10, the differentiated H9-hESC-CMs in the inhibitor group appeared more compact and resistant to dispersion during digestion. Localized contractile cell masses were disappeared.

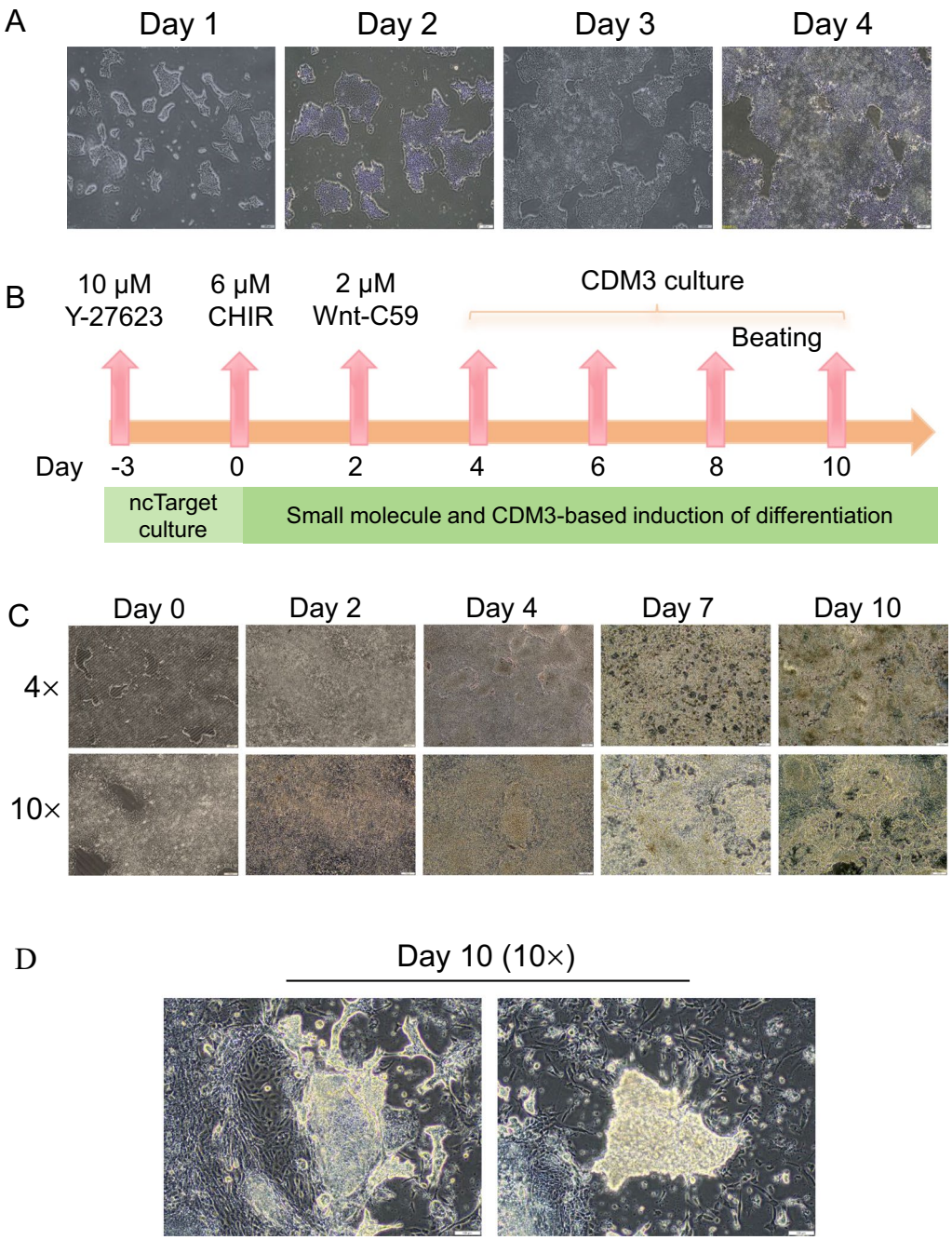

Fig. 1 Myocardial differentiation through CDM3-based methods. **A** The growth status and morphology of H9-hESCs over a period of four consecutive days under normal culture condition. It was observed that cell density reached over 80% by the fourth day, indicating the onset of myocardial differentiation in H9-hESCs. Images are representative of at least three independent experiments. Scale bar: 200 μm. **B** Timeline of cardiomyocyte differentiation derived from H9-ESCs: Following three days of culture in the ncTarget medium system, H9-hESCs initiated a 10-day differentiation process. CHIR-99021 and Wnt-C59 were added sequentially to promote the differentiation of H9-hESCs into cardiomyocytes. Cardiomyocyte survival was supported using CDM3 basal medium. **C** Cell morphology at five different time points throughout the differentiation process from H9-hESCs into cardiomyocytes observed under an optical microscope. Scale bar: 200 μm (top row); 100 μm (bottom row). **D** Local spontaneous contraction blocks in H9-hESC-CMs occasionally appeared on the tenth day of differentiation. Scale bar: 100 μm

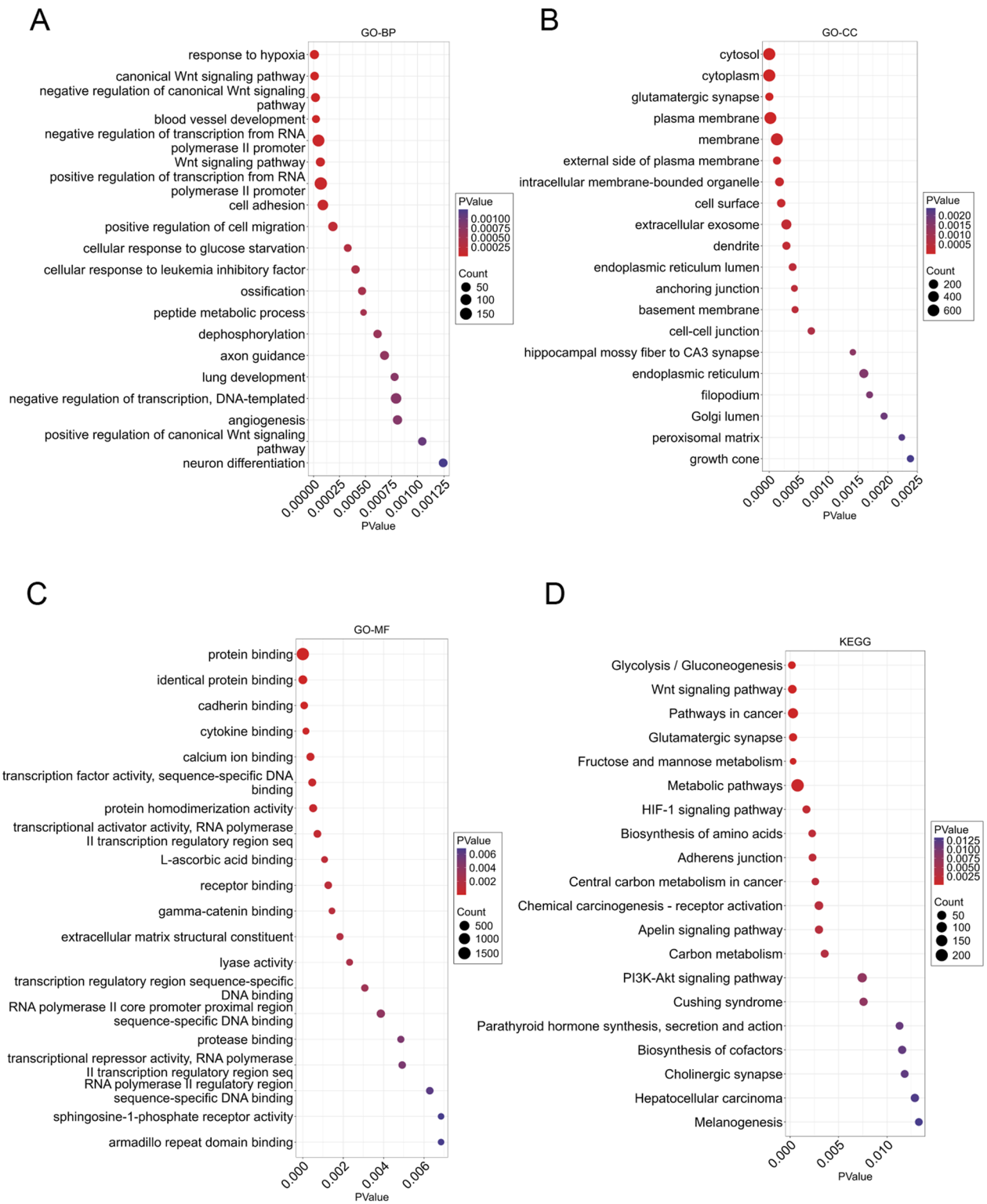

Fig. 2 Bioinformatic analysis of Wnt regulation during hESCs differentiation. GO and KEGG pathway annotations of DEGs by DAVID functional enrichment analysis provide insights into the complex roles of hESC-derived cardiomyocytes in various biological processes (BP), cellular components (CC), molecular functions (MF), and signaling pathways. **A** The first 20 significantly enriched GO annotations of BP. **B** The first 20 significantly enriched GO annotations of CC. **C** The first 20 significantly enriched GO annotations of MF. **D** The first 20 significantly enriched KEGG pathways. The size of each dot reflects the number of genes, while the color gradient of the dot indicates varying *p*-values

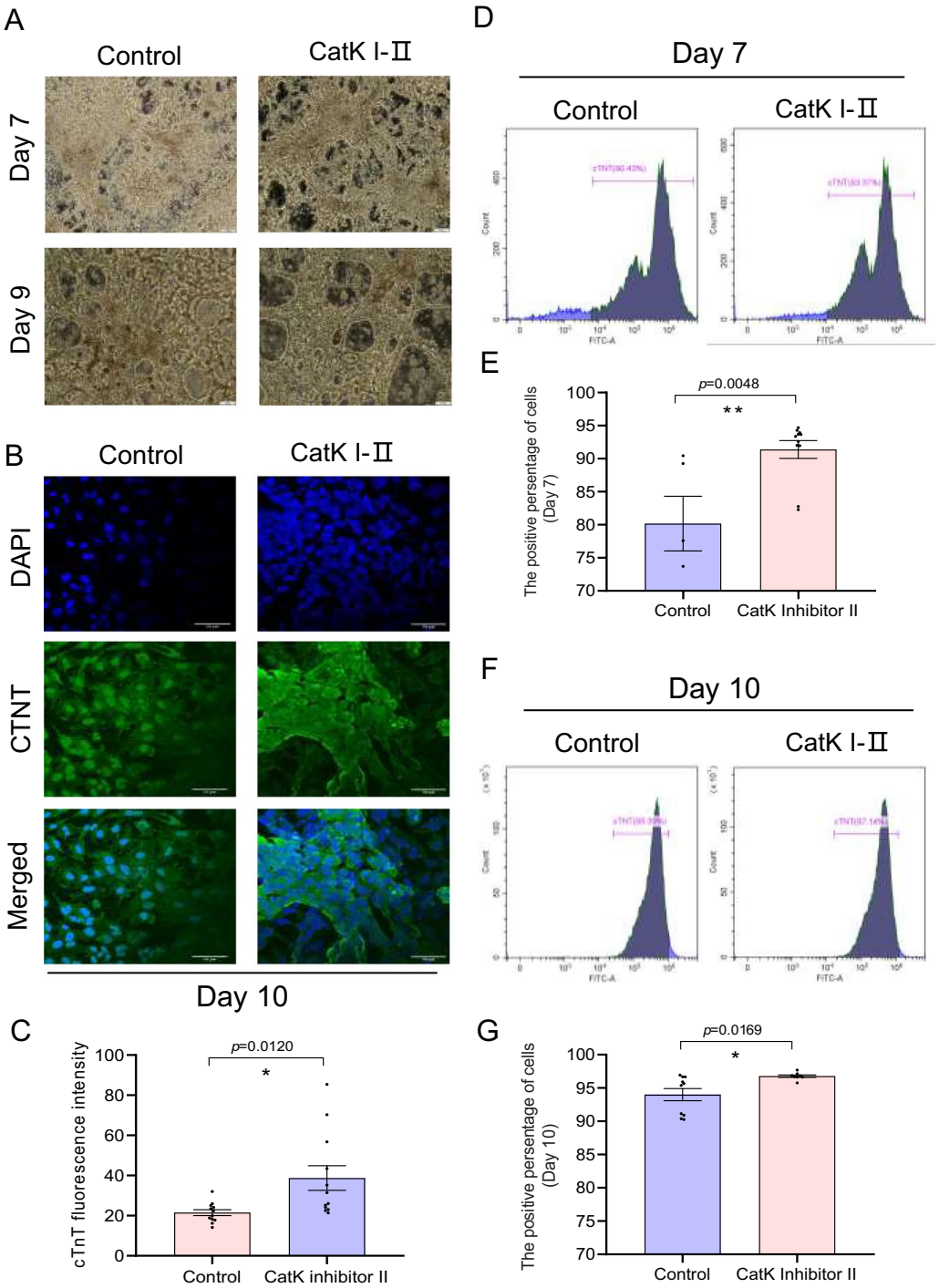

Fig. 3 The effect of cathepsin K inhibitor on the maturity of H9-hESC-CMs. **A** Representative images of contractile H9-hESC-CMs with or without cathepsin K inhibitor II on day 7 and day 9. On the seventh day of differentiation, myocardial contours were observed earlier in the cathepsin K inhibitor-treated group compared to the control group. By the ninth day, the treated group had developed a mature myocardium, characterized by a network of cells forming a ripple-like structure on top of the plated cells, indicating a more developed myocardial structure. Scale bar: 100 μm. **B** Representative immunofluorescent staining images of H9-hESC-CMs expressing cardiac troponin T (cTNT) with or without cathepsin K inhibitor II on day 10. Scale bar: 50 μm. **C** Quantification of cTNT fluorescence intensity. N = 12 images. **D** Representitive image of flow cytometry analysis of cTNT expression in H9-hESCs cultivated on Matrigel-coated plates on day 7 with or without cathepsin K inhibitor II. **E** The positive percentage of cells expressing cTNT protein. N = 5–11 indipendent treatments and measurements. **F** Representitive image of flow cytometry analysis of cTNT expression in H9-hESCs cultivated on Matrigel-coated plates on day 10 with or without cathepsin K inhibitor II. **G** The positive percentage of cells expressing cTNT protein. N = 8–10 indipendent treatments and measurements

To assess the differentiation efficiency, we examined the expression of cardiac troponin (cTNT) at different stages. Immunofluorescence and flow cytometry results revealed that cTNT expression was higher in the cathepsin K inhibitor II treatment group than that in the control group on day 7 and 10 (Fig. 3B–G). Subsequently, the stem cell pluripotency marker genes POU5F1, SOX2 and NANOG during the three stages of induction were detected (Fig. 4). Compared with control group, Cathepsin K inhibitor II significantly suppressed the expression of POU5F1 and SOX2 during early differentiation (Fig. 4A and B), decreased SOX2 and NANOG during mid-differentiation, and reduced NANOG expression at the late differentiation stage (Fig. 4B and C). Protein Levels of SOX2 and NANOG were depicted in Fig. S2, showing significant downregulation of SOX2 by the cathepsin K inhibitor II during the mid-differentiation stage (Fig. S2D and F). These findings indicated that the cell pluripotency is significantly influenced by cathepsin K inhibitor during the differentiation process. At the same time, treatment with cathepsin K inhibitor II resulted in a notable increase in the expression of cardiac transcription factor GATA4, as well as ACTN3 and MYH6 during the early differentiation (Day 2–4). Elevated expression of ACTN3, MYH6, TNNT2 and NKX2-5 were also observed at late stage (Day 8–10) induced by cathepsin K inhibitor II in comparison to the control group (Fig. 4D–H), indicating a higher mature degree of myocardial differentiation.

Cathepsin K inhibitor alters glucose metabolic profile during myocardial differentiation

In Fig. 5A, the glucose level in H9-hESCs remained high and showed no significant difference between the control and cathepsin K inhibitor group at the intial state before differentiation when neither cathepsin K inhibitor nor Wnt inhibitor was added (Day 0). However, it notably declined during cardiac mesoderm formation (Day 4) and CPCs formation (Day 7) with cathepsin K inhibitor compared to the control. No significant difference was observed between the control and inhibitor groups during cardiomyocyte maturation process (Day 10). In Fig. 5B–F, the expression levels of glycolytic metabolism genes *LDHA*, *HK2* and *SLC2A1* followed by cathepsin K inhibitor treatment were markedly decreased at the early stage of differentiation (Day 4), while *PDK1* was significantly increased compared with the control group. Furthermore, *LDHA*, *SLC2A1* and *TPL1* were remarkedly lower in cathepsin K inhibitor treatment group at the middle stage of differentiation (Day 7), indicating cathepsin K inhibitor reduces glycolysis during the transition of H9-ESCs towards cardiac mesoderm and cardiac progenitor cells. In contrast, the expression of *LDHA* and *HK2* were notably higher during the late differentiation period when cardiomyocytes reached maturity (Fig. 5B–F), suggesting glycolysis and pyruvate production are required at this stage for subsequent mitochondrial oxidative phosphorylation. These results indicated a crucial role of glucose metabolism in accelerating the differentiation and regeneration of H9-hESC-CMs by cathepsin K inhibitor.

Cathepsin K inhibitor mediates fatty acids metabolism and mitochondrial dynamics during myocardial differentiation

The gene expression of *ACACB* encoding Acetyl-CoA carboxylase (ACC) was found to be decreased followed by cathepsin K inhibitor treatment during the whole differentiation process compared with control (Fig. 6A). However, in the cathepsin K inhibitor group, *ACACB* level became higher on the tenth day than the earlier stages (Fig. 6B). Similarly, cathepsin K inhibitor reduced expression of *ACSL3* and *FABP3* on the fourth day, whereas their levels were dramatically elevated by the tenth day of the differentiation (Fig. 6C–F). In addition, *CPT1A* expression was significantly reduced at early and late stages, while *LPL* and *UCP3* were both downregulated at early and middle stages, and *UCP3* were remarkedly upregulated at late differentiation stage (Fig. S3A–B, Fig. 6G–H). The gene expression of OPA1, MFN1 and MFN2, which are essential for mitochondrial fusion, were significantly reduced during the middle stage and increased as cardiomyocytes became functional (Fig. 6I–L, Fig. S3C). *TFAM* expression was only increased significantly at the late stage (Fig. S3D). These results indicated that cathepsin K inhibitor promotes the differentiation of H9-ESCs into cardiac mesoderm and cardiac progenitor cells by reducing fatty acid metabolism, and subsequently

(See figure on next page.)

Fig. 4 The effect of cathepsin K inhibitor on the expression of stemness factors and cardiac markers of H9-hESCs during differentiation. **A**–**C** The relative mRNA level of pluripotent transcription factors *POU5F1*, *SOX2*, and *NANOG*. Cathepsin K inhibitor II restrains stem cell self-renewal. **D–F** The relative mRNA level of cardiac transcription factor *GATA4*, *ACTN3* and *MYH6*. Cathepsin K inhibitor II promotes the transition of stem cells into cardiac mesoderm. **G** and **H** The relative mRNA level of cardiac transcription factor *cTNT* and *NKX2-5*. Cathepsin K inhibitor II facilitates the maturation of cardiomyocytes. The statistical significance was assessed with the two-tailed paired t test. Mean ± SEM, n = 9, *$p < 0.05$, **$p < 0.01$, ***$p < 0.001$ to the control group

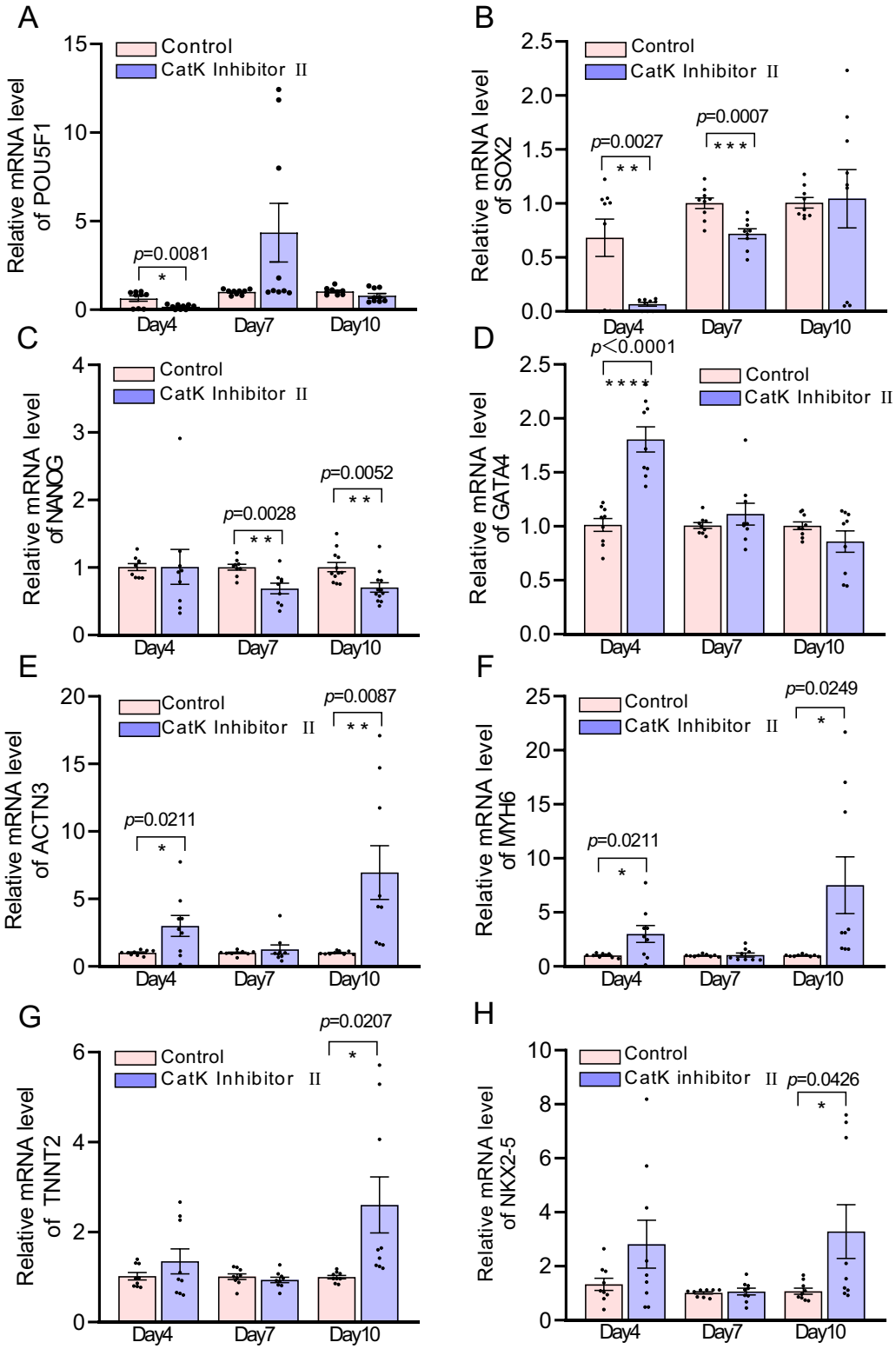

Fig. 4 (See legend on previous page.)

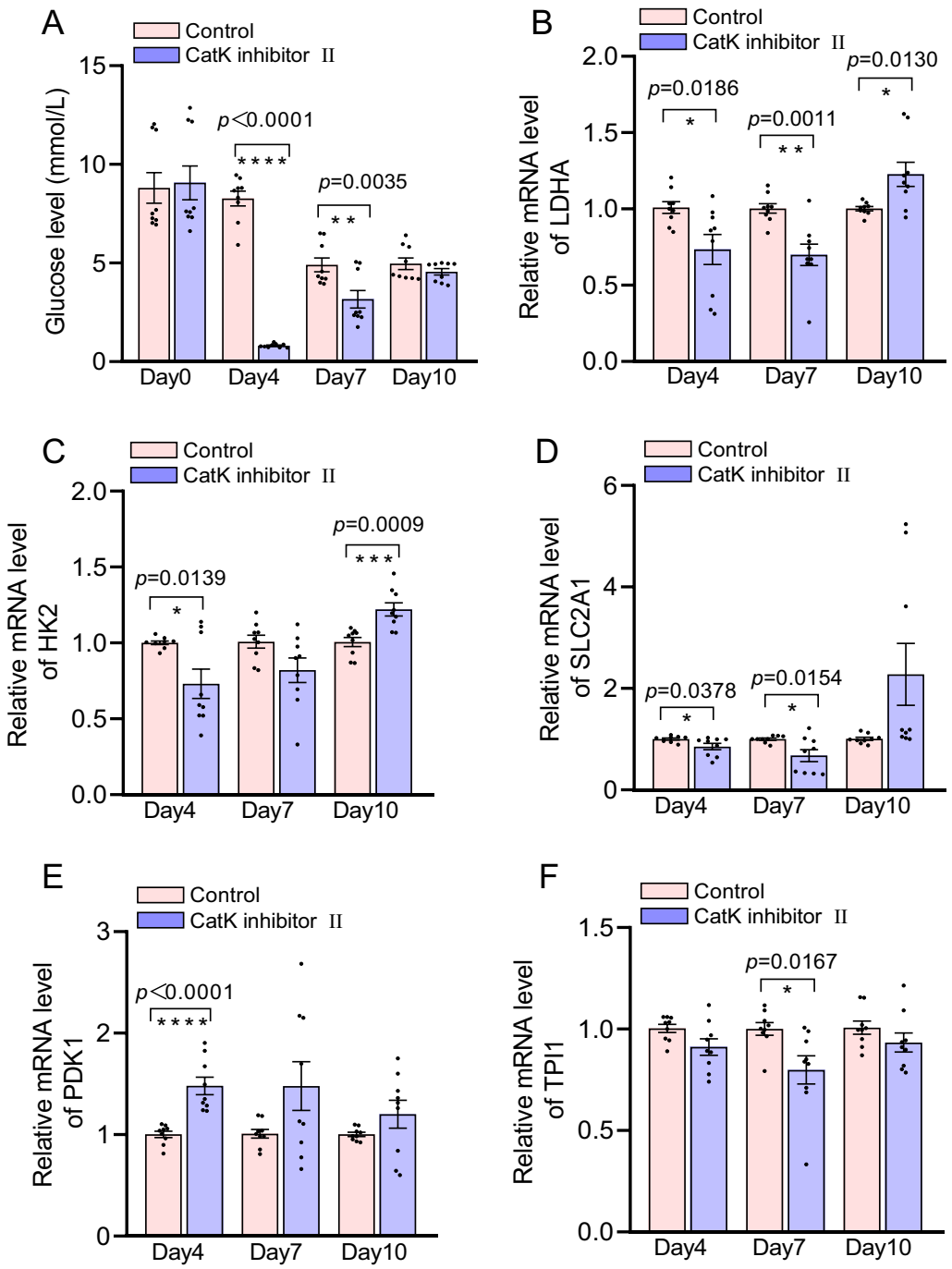

Fig. 5 The effect of cathepsin K inhibitor on the expression of glycolytic markers in H9-hESCs during differentiation. **A** In the group treated with cathepsin K inhibitor II, a decrease in glucose levels was observed during earlier stages of differentiation with mesoderm and the cardiac precursor cells formation, the levels of which were rebounded at a later stage when the cardiomyocytes began to mature, in comparison to the control group. **B–F** The relative mRNA levels of *LDHA*, *HK2*, *SLC2A1* and *PDK1* with or without cathepsin K inhibitor II revealed that cathepsin K inhibitor promoted the differentiation of H9-hESCs into mesoderm and cardiac precursor cells by reducing glycolysis, and later increasing glucose utilization when cardiomyocytes began to mature. Statistical significance was assessed with the two-tailed paired t test. Mean ± SEM, n = 9, *$p < 0.05$, **$p < 0.01$, ***$p < 0.001$, ****$p < 0.0001$ to the control group

turns to energy storge through fatty acid synthesis during the maturation of cardiomyocytes with enhanced mitochondrial fusion and biogenesis, mitochondrial DNA (mtDNA) replication and transcription.

Cathepsin K inhibitor affects PPAR-γ and apoptosis during H9-hESC-CMs differentiation

The nuclear receptor peroxisome proliferator-activated receptor γ (PPAR-γ) play vital role in cell proliferation, differentiation and apoptosis. Our results showed that cathepsin K inhibitor significantly reduced *CTSK* expression in the course of entire differentiation (Fig. 7A–B). However, *PPARG* expression was dramatically reduced only at the late differentiation stage, with no changes observed during the earlier stages (Fig. 7 C–D). Additionally, cathepsin K inhibitor obviously downregulated the expression levels of Bax and Caspase 9 at early cardiac mesoderm differentiation stage (Day 4) and late stage of differentiation (Day 10) of H9-hESC-CMs (Fig. 7E–M).

Cathepsin K Inhibitor influences mRNA level of lysosomal autophagic markers at late stage of H9-hESC-CMs differentiation

Cathepsin K inhibitor induced significant elevations in *TFEB* and *LAMP2* in H9-hESC-CMs at the late differentiation stage compared to the control (Fig. 8A–D). No significant difference was observed in the expression of *LAMP1*, *SQSTM1* and *MAP1LC3B* between cathepsin K inhibitor and control group at all different stages (Fig. 8E–J). Within cathepsin K inhibitor group, levels of *LAMP1* and *SQSTM1* were significantly reduced, while *MAP1LC3B* levels were notably increased on the tenth day compared to earlier stages (Fig. 8E–J). However, the protein levels of p62 and LC3B were not affected by cathepsin K inhibitor (Fig. S4A–I).

Discussion

H9-hESCs have the pluripotency of development and differentiation into various of cells such as nerve cells, cardiomyocytes and liver cells under specific culture conditions, providing an effective and stable source of cell regeneration in tissue damage repair. Cathepsin K belongs to cysteine protein collagenase, which is involved in cell generation, lipid and hormone expression by endocutting and degrading extracellular matrix [49]. Adult heart tissue has limited regenerative abilities**.** Efficient induction and differentiation of cardiomyocytes from stem cells can provide a stable source for cardiomyocyte regeneration, aiding in cardiovascular repair, drug toxicity screening, and various omics studies. In the present study, we demonstrated that cathepsin K inhibitor promotes the differentiation and development of H9-hESC-derived cardiomyocytes by modulating glucose and fatty acid metabolic pathways. The inhibitor accelerates cardiac mesoderm and cardiac precursor cell differentiation by decreasing glycolysis and fatty acid metabolism in early and middle stages, promoting cardiomyocyte development through enhanced autophagy, glycolysis, fatty acid anabolism and oxidative phosphorylation in later stage, thereby promoting mitochondrial fusion and biogenesis, and reduces apoptosis in H9-hESC-CMs.

Determining the optimal timing for cathepsin K inhibitor intervention during cardiomyocyte differentiation and regeneration is crucial for enhancing the yield of functional cells for treating cardiovascular diseases. The process of cardiomyogenesis from PSCs primarily entails the stepwise differentiation of mesoderm, cardiac mesoderm, and cardiac precursor cells into fully functional cardiomyocytes [50, 51]. This developmental process is tightly regulated, with various signaling pathways and transcription factors acting synergistically to orchestrate cardiac differentiation [28, 52]. In our study, we employed CDM3 medium with or without cathepsin K Inhibitor II to induce cardiomyocyte differentiation over a specified duration, and the progression of cardiomyocytes from initial morphogenesis to a relatively mature state of contractile function was successfully achieved, aligning with findings from previous studies. For instance, Tan et al. cultured hiPSCs and noted spontaneous cell mass contractions approximately 8 days post-differentiation [53]. Similar to Fu et al. and Tan et al.'s method, we selected the Wnt pathway to direct hESCs towards mesodermal differentiation. CHIR99021 was initially used to activate Wnt pathway. After 48 h, the small molecule antagonist Wnt-C59 was applied to induce the transition to CPCs. The intervention was then halted with CDM3 basal

(See figure on next page.)

Fig. 6 The effect of cathepsin K inhibitor on fatty acids metabolism and mitochondrial fusion factors in H9-hESCs during differentiation. **A** and **B** The relative mRNA level of *ACACB* with or without cathepsin K inhibitor II. **C** and **D** The relative mRNA level of *ACSL3* with or without cathepsin K inhibitor II. **E** and **F** The relative mRNA level of *FABP3* with or without cathepsin K inhibitor II. **G** and **H** The relative mRNA level of *UCP3* with or without cathepsin K inhibitor II. **I** and **J** The relative mRNA level of *MFN1* with or without cathepsin K inhibitor II. **K** and **L** The relative mRNA level of *MFN2* with or without cathepsin K inhibitor II. These results showed that fatty acid metabolism and mitochondrial fusion were suppressed at the early and/or mid-stages of differentiation by cathepsin K inhibitor, and were increased at the later stage. Statistical significance was assessed with the two-tailed paired t test. Mean ± SEM, n = 9–12, *$p < 0.05$, **$p < 0.01$, ***$p < 0.001$, ****$p < 0.0001$ to the control group

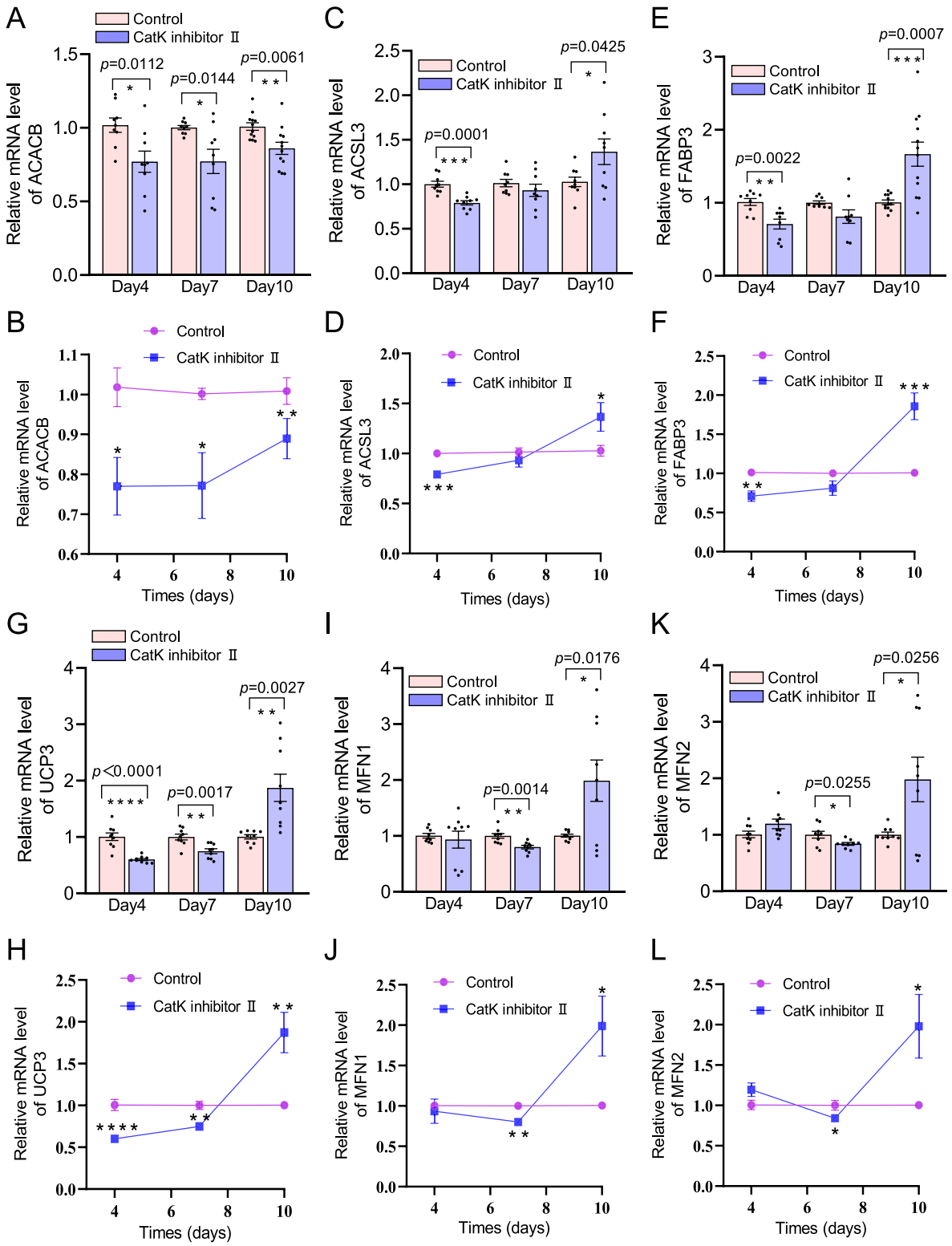

Fig. 6 (See legend on previous page.)

medium, and the culture was maintained until the cardiomyocytes matured [54]. Comparably, Kehat et al., utilizing suspension culture of stem cells, observed embryoid bodies displaying ultrastructural myofibril bundles and functional properties resembling early cardiomyocytes' contractile characteristics by day 10 [55]. Although the hanging drop method has lower nutrient consumption, cell aggregation is not stable, as well as the uneven embryoid body formation and size may result in inconsistent differentiation efficiency [56]. Researchers using the GiWi2 induction method also reported the initial spontaneous contraction wave by day 7 and robust myocardial beats by day 10 [57]. Due to the heterogeneity of the hanging drop method and the complexity of regulating pluripotent transcription factors using the GiWi2 method, we selected the CDM3 culture method for efficient short-term differentiation of hESCs. Furthermore, akin to studies on hESC-CMs [58] and iPSC-CMs differentiation [59], H9-hESC-CMs initially showed a short, round morphology during early differentiation. After ten days of differentiation, cells developed into a rod-like, spindle-shaped, or inverted triangle structure resembling human AC16 ventricular cardiomyocytes, observed in the central region of the cell culture dish.

In the presence of cathepsin K Inhibitor II, the number of cells began to increase and converged with each other on the fourth day of the induction culture. On the seventh day of differentiation, the aggregated cells started to produce numerous local clusters of spontaneously beating cardiomyocytes. During the late stage of differentiation, as mitochondria underwent biogenesis and structural integration, cardiomyocytes began to establish a stable contractile cell layer observable under an inverted microscope. By the ninth day, a prominent surface layer of cells displaying robust and uniform rhythmic myocardial contractions became noticeable. The cathepsin K inhibitor facilitated the differentiation and maturation of cardiomyocytes, as evidenced by significantly reduced pluripotency markers and increased expression of cardiac transcription factors such as *GATA4* and *NKX2.5*, along with increased *TNNT2*/c-TNT, *ACTN3*, and *MYH6* during cardiac differentiation. These findings suggest that the cathepsin K inhibitor may hold significant research implications for enhancing stem cell applications in human cardiac development, drug screening, toxicity testing, functional genomics and cardiac injury repair [60]. Nevertheless, specific criteria such as sorting and culturing of H9-hESC-CMs, as well as assessing functional contraction, still require extended purification culture and further in-depth exploration.

Stem cells exhibit distinct metabolic characteristics from other cells, which influence tissue homeostasis and regeneration [61]. Throughout the differentiation process of cardiomyocytes induced by stem cells, there occurs a metabolic shift from glycolysis to oxidative phosphorylation, involving multiple overlapping molecular mechanisms of metabolic reprogramming in the process of cardiomyogenesis [62]. Glis1-induced glycolytic flux, intracellular α-ketoglutarate levels or its ratio to succinate are critical in governing the stemness and differentiation state of PSCs, thereby mediating a connection between cellular epigenome and metabolomics [63–65]. Our results revealed that cathepsin K inhibition suppressed glycolysis as indicated by reduced cellular glucose level, notably decreased expression of *LDHA*, *HK2*, *SLC2A1*, *TPI1* and increased *PDK1* during early and middle stages of differentiation compared to the control group, implying diminished conversion capacity of lactate, pyruvate, and acetyl-CoA during these stages. These were also supported by the previous studies that high glucose inhibits neural stem cell differentiation [66], *LDHA* and *HK2* promote cell proliferation and maintain stem cell stemness [67–70]. At the same time, lipid metabolism was also hindered by cathepsin K inhibitor as shown as decreased levels of *ACACB*, *ACSL3*, *LPL*, *FABP3,* and *CPT1A*, presumably due to the decreased glycolytic metabolism and intracellular energy under cathepsin K inhibitor treatment, which accelerated the differentiation progression from mesoderm to cardiac mesoderm and onward to cardiac precursor cells. In contrast, cathepsin K inhibition significantly boosted the expression of *LDHA*, *HK2*, *SLC2A1*, *ACSL3*, and *FABP3*, while keeping *ACACB* and *CPT1A* at lower levels during the later stages of differentiation, causing differentiated cardiomyocytes to utilize more glucose and fatty acids as their primary energy sources, as compared to the control. This indicates that

(See figure on next page.)

Fig. 7 The effect of cathepsin K inhibitor on PPAR-γ and apoptotic markers during H9-hESC-CMs differentiation. **A** and **B** The relative mRNA level of *CTSK*. **C** and **D** The relative mRNA level of *PPARG*. **E** Representative bands of Caspase 9, GAPDH and BAX on day 4. **F** and **G** Normalized protein level of Caspase 9 and BAX in cells by Western Blot analysis on day 4. **H** Representative bands of Caspase 9, GAPDH and BAX on day 7. **I** and **J** Normalized protein level of Caspase 9, GAPDH and BAX in cells by Western Blot analysis on day 7. **K** Representative bands of Caspase 9, GAPDH and BAX on day 10. **L** and **M** Normalized protein level of Caspase 9 and BAX in cells by Western Blot analysis on day 10. These results revealed that cathepsin K inhibition reduced pro-apoptotic markers and PPAR-γ mRNA level at early and/or late stages of differentiation, with no significant changes observed during the middle stage. Statistical significance was assessed with the two-tailed paired t test. Mean ± SEM, n = 9–12, *$p < 0.05$, **$p < 0.01$, ***$p < 0.001$, ****$p < 0.0001$ to the control group

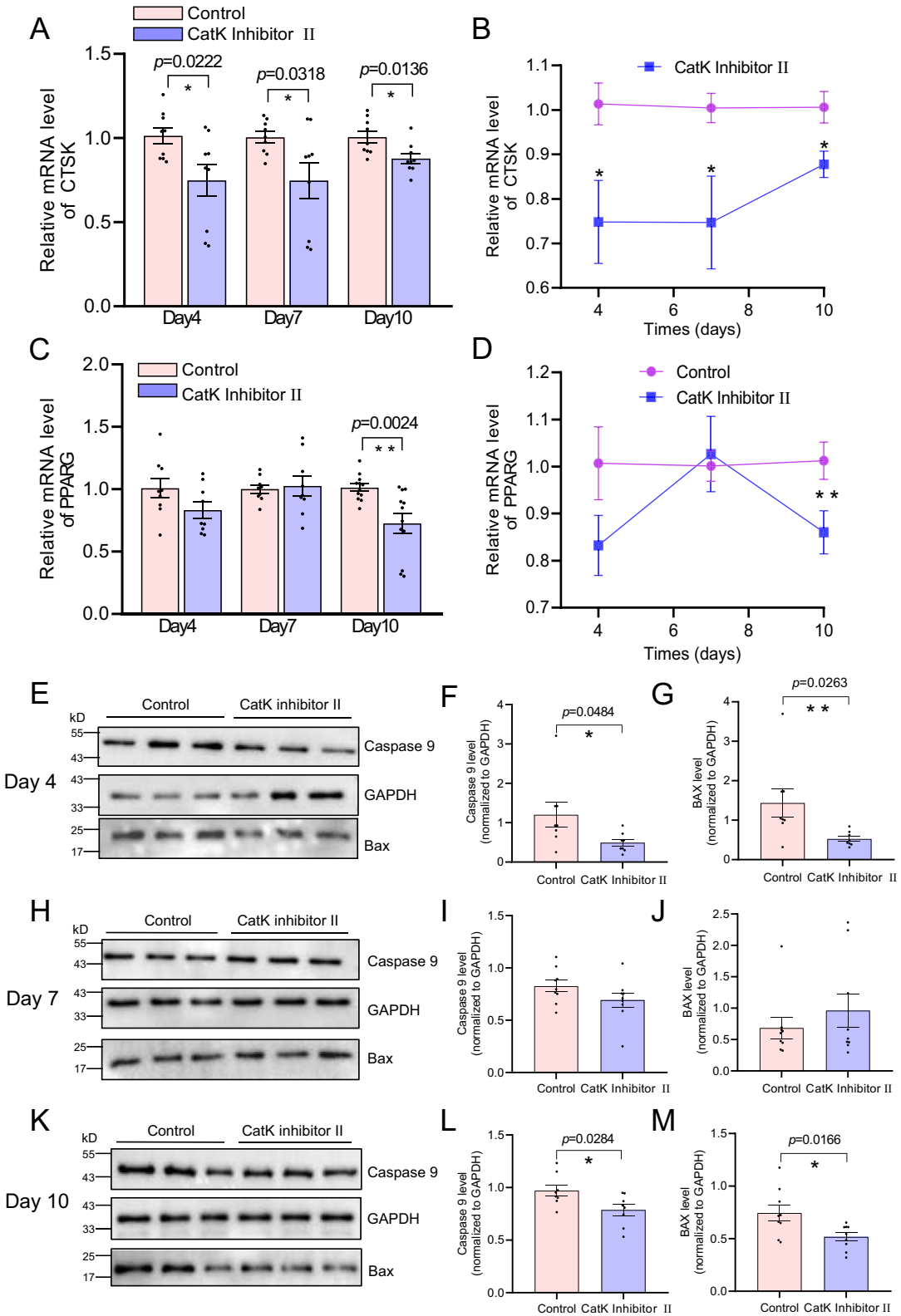

Fig. 7 (See legend on previous page.)

during this phase, inhibiting cathepsin K promotes the generation and conversion of pyruvate, fatty acid metabolism and oxidative phosphorylation, thereby enhancing energy production for the development and maturation of cardiomyocytes. However, the elevated UCP3 and reduced PPAR-γ suggests a higher supply of fatty acids to the mitochondria than their oxidation capacity, meanwhile lowering oxidative stress burdern and apoptosis as evidenced by reduced Bax and Caspase 9. Increased fatty acid synthesis enables binding to FABP3 for nuclear transport and storage as energy reserves. Upregulated mitochondrial UCP3 and reduced CPT1 are essential to balance fatty acid oxidation for glucose uptake/utilization. Meanwhile, CPT1 is a key enzyme facilitating carnitine-dependent transport across the mitochondrial inner membrane. Its deficiency can hinder cell proliferation [71].

Mitochondria serve as the powerhouse of cellular activities and are predominantly found in various types of muscle tissues with contractile functions. As cardiomyocytes differentiate from PSCs, mitochondrial morphology transitions from fragmented structures to larger organelles capable of generating sufficient ATP to support cardiac contractile function [25]. When mitochondrial structure is compromised, the cell fate of neural stem cells can be influenced by alterations in metabolic and physiological characteristics [72]. In our present study, the early cell morphology was primarily characterized by germ layer transitions, with no significant changes in the expression of mitochondrial double membrane fusion genes. However, during the mid-stage of differentiation, there was a notable decrease in the expression of mitochondrial fusion genes of cells following Cathepsin K inhibition. This suggests that during this stage, cellular regulation primarily involves mesodermal differentiation into cardiac precursor cells, with fewer mitochondrial fusion events. Mitochondria are mainly present in the cytoplasm. At the late differentiation stage of cardiomyocytes, as glucose and fatty acid metabolism increased, cardiomyocytes dominantly obtain energy through oxidative phosphorylation and promoted mitochondrial biogenesis and bilayer fusion evidenced by increased *TFAM*, *OPA1*, *MFN1* and *MFN2*. Newly fused functional mitochondria are mainly distributed in the myofibrils of cardiomyocytes to provide energy for the beating of cardiomyocytes. This aligns with the conversion of metabolic substrates from glucose, a hallmark of cardiomyocyte maturation, to fatty acids, which can enhance mitochondrial respiratory reserve capacity and improve myocardial contractility [73]. Co-culturing newborn cardiomyocytes with stem cells has also been shown to notably enhance cardiomyocyte area, sarcomeric length, and mitochondrial copy number during the later stages of differentiation [74].

Cathepsin K, the most potent cysteine protease in mammalian lysosomes, plays a crucial role in preserving lysosomal function and cellular metabolism, and has been implicated in apoptosis regulation [75, 76]. The lysosome serves as a central hub for intracellular cargo transport and signal transduction, playing a crucial role in regulating metabolic pathways within mammalian cells [77]. Our results revealed that during the mesodermal transition and primary differentiation stages of cardiac precursor cells, the cathepsin K inhibitor did not significantly alter autophagosome generation and lysosomal autophagic flow. However, the expression of LAMP2 and TFEB which are involved in autophagosome maturation, autophagic flux, and lysosomal biogenesis were remarkedly increased during the late differentiation stage compared to control group, without affecting the levels of LAMP1, p62, and LC3. This suggests that the lysosomal function and autophagic flux are enhanced in H9-hESC-CMs by cathepsin K inhibition, which may contribute to cell signal transduction, energy conversion and intracellular homeostasis to maintain normal life activities in cardiomyocytes.

Although our study provides important insights into the role of cathepsin K inhibitior II in hESC-CMs, several limitations exist. First, we only utilized H9-hESCs as an in vitro model, and it is unclear whether the results are applicable to other types of PSCs (e.g. hiPSCs). Therefore, future studies should further investigate the differential responses of various stem cell types to cathepsin K inhibitors. Despite the experimentally demonstrated beneficial effects of cathepsin K inhibitior on hESC-CMs, its efficacy and safety have not yet been systemcally validated in

(See figure on next page.)

Fig. 8 The effect of cathepsin K inhibitor on lysosomal autophagy during H9-hESC-CMs differentiation. **A**–**B** The relative mRNA level of *TFEB* with or without cathepsin K inhibitor II. **C** and **D** The relative mRNA level of *LAMP2* with or without cathepsin K inhibitor II. **E** and **F** The relative mRNA level of *LAMP1* with or without cathepsin K inhibitor II. **G** and **H** The relative mRNA level of *SQSTM1* with or without cathepsin K inhibitor II. **I** and **J** The relative mRNA level of *MAP1LC3B* with or without cathepsin K inhibitor II. These results showed that levels of lysosomal autophagy markers *TFEB* and *LAMP2* were both increased by cathepsin K inhibitor at the late differentiation stage, without significant alterations in *SQSTM1* and *MAPILC3B* when compared to the control. Statistical significance was assessed with the two-tailed paired t test. Mean ± SEM, n = 6–12, $*p < 0.05$ to the control group

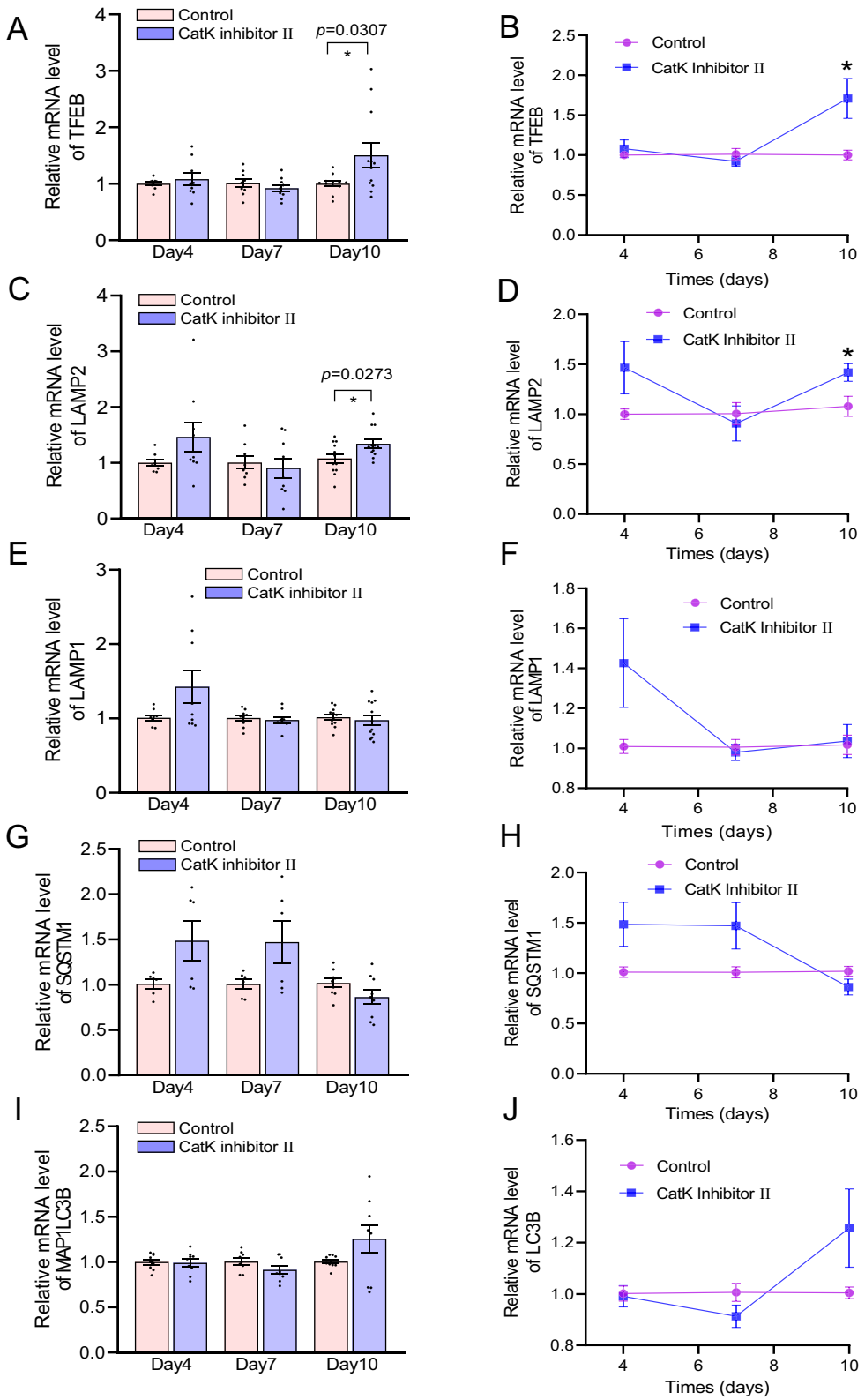

Fig. 8 (See legend on previous page.)

animal models or preclinical applications. Furthermore, the impact of cathepsin K deficiency in PSC-CMs on cardiac regeneration and repair in animal models, as well as its potential for clinical translation, require further investigation.

Summary and conclusion

To sum up, in the presence of a cathepsin K inhibitor, hESCs transitioning to cardiac mesoderm and cardiac precursor cells at the early and mid-differentiation stages primarily produce short, round, functionally immature cardiomyocytes with a modest number of mitochondria. This is achieved by reducing glycolysis and fatty acid metabolism, downregulating apoptotic proteins, and preserving mitochondrial membrane integrity with fewer fusion events. During the mid to late differentiation stages, cardiomyocytes exhibit spontaneous contraction and beating. H9-hESC-CMs develop primarily through oxidative phosphorylation, utilizing glucose and fatty acids as main energy sources to generate more ATP and mature into cardiomyocytes with larger, more intact mitochondria, facilitated by increased mitochondrial fusion. Additionally, lysosomal autophagy is activated, and apoptosis remains lower, ensuring the proper functioning of cardiomyocytes.

In conclusion, our study indicates that inhibiting cathepsin K enhances the differentiation of hESCs into functional cardiomyocytes by regulating glucolipid metabolism and mitochondrial maturation. This process is linked to the changes in mitochondrial fusion and biogenesis, apoptosis, and lysosomal autophagy, which are crucial for H9-hESC-CMs to maintain a balance between energy storage and utilization during different differentiation stages.

Prospect

This study provides a new theoretical basis for further understanding the relationship between cathepsin K and cardiomyocyte differentiation, which may provide more numbers of renewable cell sources for the repair of cardiac tissue damage in different cardiovascular diseases. It also provides a potential research direction for the clinical application and scientific transformation of cardiomyocytes differentiation and regeneration. Since cardiac regeneration can be achieved by changing the energy metabolism of cardiomyocytes, further in-depth studies are needed to elucidate the link between the related signal transductional molecues involved in the occurrence of glucolipid metabolism and myocardial repairment in the course of stem cell therapy. With the optimal cell signaling molecules and a 3D environment, ESCs could potentially develop into organoids in engernered culture dishes, and may one day be used for organ transplantation.

Materials and methods

Cell lines

H9-hESCs were obtained from the Research Center for Eco-Environmental Sciences of Chinese Academy of Sciences. Cells were cultured in complete ncTarget hPSC Mediun (RP01020, Nuwacell Biotechnologies Co., Ltd., Hefei, China) supplemented with 1% penicillin–streptomycin (SC120-01, Seven Biotech Co., Ltd., Beijing, China) and incubated in an incubator with 5% CO_2 at 37 °C. H9-hESCs were then expanded on 0.6% Matrigel matrix-coated (BD356231, Corning®) plates for subsequent experiments.

Differentiation of H9-hESCs into myocardial cells

H9-hESCs were preincubated with 10 μM ROCK inhibitor Y-27632 (HY11071, MCE®) for 24 h. When cells reached 80% confluence (Day 0), they were fed by CDM3 basal medium supplemented with 6 μM CHIR99021 (HY-10182, MCE®) in Matrigel matrix-coated 6-well culture plates. After 48 h, the medium was replaced with CDM3 supplemented with 2 μM Wnt-C59 (HY-15659, MCE®). On the fourth day of the culture cycle (Day 4), the cells were transitioned to basal CDM3 medium composed of RPMI 1640 basal medium (C11875500BT, Gibco™), 213 μg/mL L-AA2P (SLCC4552, Sigma-Aldrich®), 500 μg/mL BSA (WXBD0065V, Sigma-Aldrich®) and 1% penicillin–streptomycin (SC120-01, Seven Biotech Co., Ltd., Beijing, China) until the completion of differentiation on day 10.

Bioinformatic screening of key DEGs and functional pathways during cardiac differentiation

We used the keywords "hESCS, differentiation, induction and cardiomyocytes" to search for the data for gene expression profiles. We opted for the GSE67154 dataset due to its alignment with the differentiation time point and the testing methodology. This dataset captures the precise time course of Wnt signaling-induced cardiomyocyte differentiation along the mesodermal pathway. The samples treated with the differentiation inducing factors FGF2, BMP4, CHIR00921 and WNT inhibitor IWP-2 were defined as the FBW group. The samples treated with the factors FGF2, BMP4 and CHIR00921were defined as the FB group. Each of the FBW and FB groups consists of four samples. Samples from differentiation time points on days 2, 4, 6, and 8 in the GSE67154 dataset were chosen for further analysis by GEO2R (https://www.ncbi.nlm.nih.gov/geo/geo2r/). Genes that met the cutoff criteria of the p-value < 0.05 and |log2 FC| > 1 were considered differentially expressed genes (DEGs). The

GO (Gene Ontology) and KEGG (Kyoto Encyclopedia of Genes and Genomes) enrichment analyses were carried out to predict the potential functions of the DEGs by using the database for annotation, visualization, and integrated discovery (DAVID; https://david.ncifcrf.gov/). The significant biological functions and pathway enrichment were defined based on criteria set at p-value < 0.05. We used the R software (Version 4.3.2) to visualize the top 20 enrichment results.

Cathepsin K inhibitor treatment

During the process of H9-hESCs differentiation into cardiomyocytes, either 1 μM of Cathepsin K inhibitor II (219,379, Sigma-Aldrich®) or vehicle (0.1% DMSO, #D8371, Solarbio®) was added to the cells on day 2, day 5 and day 8. Samples were collected after 48 h of the treatment.

Glucose assay

The cellular glucose level was measured using a glucose assay kit (A154-1-1, Nanjing Jiancheng Bioengineering Institute, Nanjing, China) according to the manufacturer's protocols. The principle of glucose oxidase involves the formation of a reddish-purple pigment upon glucose reaction. The absorbance of this pigment is measured at 505 nm using a microplate reader (SpectraMax iD3, MOLECULAR DEVICES, Shanghai, China), with the color intensity being directly proportional to the glucose concentration in the sample.

Flow cytometric analysis

The expression of cardiac troponin T (cTnT) in differentiated cardiomyocytes was evaluated using the cTnT primary antibody (1:500, 15,513-1-AP, Proteintech Group Inc.) and anti-mouse flow cytometric (FC) secondary antibody (1:200, SA00013-2, Proteintech Group Inc.) through a flow cytometer (CytoFLEX, Beckman Coulter). A 488 nm fluorescence channel was selected to identify the target protein antibody, allowing for the measurement of the positive percentage of the cells. The positive gate boundary was set using a non-specifically labeled negative control, and the fluorescence intensity was measured with 10,000 cells per experimental group. The data were analyzed using CytExpert software, version 2.4 (CytExpert, Beckman Coulter, California, USA). The quantification results were statistically analyzed using a t-test to compare the differences between groups. At least three independent experiments were performed.

Immunofluorescence (IF) staining

The cells were fixed with 4% paraformaldehyde (G1101, Servicebio Technology Co., Ltd., Wuhan, China) for 15 min at room temperature, followed by permeabilization with 0.2% Triton X-100 in PBS for 10 min. After fixation, the cells were blocked with normal goat serum (SL038, Solarbio®) for 1.5 h at room temperature. Subsequently, they were incubated with the cTnT primary antibody (1:500, 15,513–1-AP, Proteintech Group Inc.) diluted in 1% BSA at 4 °C overnight. After extensive washing with PBS, the slides were incubated with anti-mouse secondary antibody (1:200, SA00013-2, Proteintech Group Inc.) followed by nuclear staining with DAPI. Imaging was conducted at room temperature using a laser scanning confocal microscopy (Olympus FV-3000) equipped with a 40× objective. Fluorescence of DAPI was captured with an excitation wavelength at 360 nm and an emission wavelength at 460 nm. Fluorescence of the secondary antibody was excited with an excitation wavelength at 488 nm and an emission wavelength at 515 nm. The fluorescence intensity of cTNT was quantified by using Image J software (Fiji, National Institutes of Health, Bethesda, MD, USA).

Primer design, total RNA extraction, cDNA synthesis, reverse transcription, and real-time PCR

Total RNA was isolated from H9-hESC-CMs samples using the TRIzol reagent (DP424, TIANGEN Biotech Co., Ltd., Beijing, China), followed by DNase digestion to eliminate genomic DNA contamination. RNA was quantified using a NanoDrop 2000c spectrophotometer (Thermo Fisher Scientific). Synthesis of cDNA and reverse transcription was performed using 1 μg total RNA in a 10-μl system following the instructions of FastQuant RT Kit first strand synthesis kit (KR116-02, TIANGEN Biotech Co., Ltd., Beijing, China). Primers in this study were designed by using the Nucleotide BLAST tool on National Center for Biotechnology Information (NCBI) website (https://blast.ncbi.nlm.nih.gov/Blast.cgi) and were referenced from previously published studies [78, 79]. The quantitative real-time PCR was detected by a C1000 Touch Thermal Cycler CFX96TM Real-Time System (Bio-Rad) per the iQTM SYBR® Green Supermix (Bio-Rad) instructions. Relative mRNA expression levels for each gene were determined by using the $2^{-\Delta\Delta Ct}$ method. *GAPDH* was used as reference internal standard. Each group was subjected to three independent experiments, with three replicates for each sample. The primer sequences are shown in Table S1.

Protein extracting and Western blot analysis

Total protein was extracted in RIPA (R0020, Solarbio®) lysis buffer and quantified by using a BCA kit (PC0020, Solarbio®) and a Microplate reader (Molecular Devices, Silicon Valley, CA, USA). Cell lysates with loading buffer (01411, CoWin Biotech Co., Ltd., Jiangsu, China) was preheated at 95 °C for 5 min. Protein samples were separated

by sodium dodecyl sulphate (SDS)-polyacrylamide gels, and transferred electrophoretically to Immobilon® PVDF membranes (ISEQ00010, Merck) in the Tris/glycine transfer buffer (25 mM Tris, 192 mM glycine, 20% methanol). The membranes were blocked with 5% milk in TBS-T for 1 h at room temperature. After washing with TBS-T for three times, membranes were incubated overnight at 4 °C with anti-SOX2 (1:1000, PTM-5072, PTM Biolabs Inc.), NANOG (1:1000, PTM-6010, PTM Biolabs Inc.), LC3B (1:1000, CST3868, Cell Signaling Technology™), SQSTM1/p62 (1:1000, CST5114S, Cell Signaling Technology™), Bax (1:1000, CST2772S, Cell Signaling Technology™), Caspase 9 (1:1000, PTM-5311, PTM Biolabs Inc.) and GAPDH (1:1000, 60,004-1-Ig, Proteintech Group Inc.) primary antibodies. Blots were incubated with horseradish peroxidase (HRP)-conjugated secondary antibody (1:5000) for 1 h at room temperature. Antigens were detected by the luminescence method. Images were captured through ChemiDoc Touch Imaging System (Bio-Rad) with ECL (PK10003, Proteintech Group Inc.). Band densities were determined using Image Lab software (version 5.1, Bio-Rad).

Statistical analysis

Statistical analysis was performed using GraphPad Prism 9 software. For each experiment, we performed at least three independent biological repetitions. Data were presented as mean ± SEM. The Shapiro–Wilk normality test was used to analyze normal (Gaussian) distribution. Statistical significance ($^{*}p < 0.05$, $^{**}p < 0.01$, $^{***}p < 0.001$, $^{****}p < 0.0001$) for each variable was estimated by an unpaired t-test (two-tailed) or a one-way analysis of variance (ANOVA) followed by a Tukey's post hoc analysis.

Supplementary Information

The online version contains supplementary material available at https://doi.org/10.1186/s13287-025-04231-7.

Additional file1
Additional file2
Additional file3
Additional file4
Additional file5
Additional file6
Additional file7
Additional file8
Additional file9

Acknowledgements
We acknowledge professor Francesco Faiola from Research Center for Eco-Environmental Sciences, Chinese Academy of Sciences for kindly providing us the H9-hESCs. This work was funded by the National Natural Science Foundation of China (32171181, R.G.), the Beijing-Tianjin-Hebei Basic Research Cooperation Special Project and the Hebei Natural Science Foundation (J230018: H2023201901, R.G.), and the Interdisciplinary Research Program of Natural Science of Hebei University (DXK202105, R.G.). The authors declare that they have not use AI-generated work in this manuscript.

Significance statement
The efficient differentiation and the quality of cardiomyocytes are crucial for the repair of damaged myocardium. The study highlights the significant impact of cathepsin K inhibition on the differentiation of human embryonic stem cells (H9-hESCs) into functional cardiomyocytes. By applying a cathepsin K inhibitor during specific stages of myocardial differentiation, we observed enhanced cardiomyocyte generation with improved mitochondrial integrity and energy metabolism. The inhibition of cathepsin K accelerated early differentiation and optimized metabolic processes, leading to more mature and functionally robust cardiomyocytes. This approach not only promotes effective cardiac tissue regeneration but also opens new avenues for enhancing cardiac repair through targeted molecular interventions.

Author contributions
Y.W. and R.G. conceived and designed research; Y.W., Y.C. and X.L. conducted experiments, analyzed and interpreted the data; Y.W. wrote the original draft. S.L provided techniques and experimental validation; L.Z. provided project management and resources. R.G. provided fundings, resources and expertise, supervised the experiments, review and revised the manuscript.

Availability of data and materials
The data generated or analyzed during the current study are included in the manuscript or available from the online supplemental materials. The RNA-seq dataset supporting the results in this article can be found in the Gene Expression Omnibus (GEO) repository under the accession number GSE67154. The dataset can be accessed at http://www.ncbi.nlm.nih.gov/geo/query/acc.cgi?acc=GSE67154.

Declarations

Ethics approval and consent to participate
H9-hESCs were generously obtained from the Research Center for Eco-Environmental Sciences under the Chinese Academy of Sciences. The protocol was approved by the Hebei University Animal Welfare and Ethical Committee (Project: Role of Cathepsin K in the Development of Diabetic Atherosclerosis by regulating SERCA2-SUMOylation. No. IACUC-2021XG032, approved on Mar. 11, 2021).

Competing interests
The authors declare no competing financial interests.

Author details
[1]College of Life Sciences, Institute of Life Science and Green Development, Hebei University, Baoding 071002, China. [2]College of Osteopathic Medicine of the Pacific, Western University of Health Sciences, Pomona, CA 91766, USA. [3]The Key Laboratory of Zoological Systematics and Application, College of Life Sciences, Hebei University, Baoding 071002, China.

Received: 21 October 2024 Accepted: 14 February 2025
Published online: 05 March 2025

References

1. Costantino S, Paneni F, Cosentino F. Ageing, metabolism and cardiovascular disease. J Physiol. 2016;594:2061–73.
2. Sun Y, Liu J, Xu Z, Lin X, Zhang X, Li L, Li Y. Matrix stiffness regulates myocardial differentiation of human umbilical cord mesenchymal stem cells. Aging (Albany NY). 2020;13:2231–50.
3. Abou-Saleh H, Zouein FA, El-Yazbi A, Sanoudou D, Raynaud C, Rao C, Pintus G, Dehaini H, Eid AH. The march of pluripotent stem cells in cardiovascular regenerative medicine. Stem Cell Res Ther. 2018;9:201.
4. Tani H, Tohyama S, Kishino Y, Kanazawa H, Fukuda K. Production of functional cardiomyocytes and cardiac tissue from human induced

pluripotent stem cells for regenerative therapy. J Mol Cell Cardiol. 2022;164:83–91.
5. Li L, Wan Z, Wang R, Zhao Y, Ye Y, Yang P, Qi Y, Jiang W, Cai L, Zhang D. Generation of high-performance human cardiomyocytes and engineered heart tissues from extended pluripotent stem cells. Cell Discov. 2022;8:105.
6. Kolios G, Moodley Y. Introduction to stem cells and regenerative medicine. Respiration. 2013;85:3–10.
7. Samak M, Hinkel R. Stem cells in cardiovascular medicine: historical overview and future prospects. Cells. 2019;8:1530.
8. Barad L, Schick R, Zeevi-Levin N, Itskovitz-Eldor J, Binah O. Human embryonic stem cells vs human induced pluripotent stem cells for cardiac repair. Can J Cardiol. 2014;30:1279–87.
9. Choi YS, Dusting GJ, Stubbs S, Arunothayaraj S, Han XL, Collas P, Morrison WA, Dilley RJ. Differentiation of human adipose-derived stem cells into beating cardiomyocytes. J Cell Mol Med. 2010;14:878–89.
10. Ni J, Sun Y, Liu Z. The potential of stem cells and stem cell-derived exosomes in treating cardiovascular diseases. J Cardiovasc Transl Res. 2019;12:51–61.
11. Feyen DAM, Gaetani R, Doevendans PA, Sluijter JPG. Stem cell-based therapy: improving myocardial cell delivery. Adv Drug Deliv Rev. 2016;106:104–15.
12. Cyranoski D. How human embryonic stem cells sparked a revolution. Nature. 2018;555:428–30.
13. Tachibana M, Amato P, Sparman M, Gutierrez NM, Tippner-Hedges R, Ma H, Kang E, Fulati A, Lee HS, Sritanaudomchai H, Masterson K, Larson J, Eaton D, Sadler-Fredd K, Battaglia D, Lee D, Wu D, Jensen J, Patton P, Gokhale S, Stouffer RL, Wolf D, Mitalipov S. Human embryonic stem cells derived by somatic cell nuclear transfer. Cell. 2013;153:1228–38.
14. Cao N, Liu Z, Chen Z, Wang J, Chen T, Zhao X, Ma Y, Qin L, Kang J, Wei B, Wang L, Jin Y, Yang HT. Ascorbic acid enhances the cardiac differentiation of induced pluripotent stem cells through promoting the proliferation of cardiac progenitor cells. Cell Res. 2012;22:219–36.
15. Parrotta EI, Lucchino V, Scaramuzzino L, Scalise S, Cuda G. Modeling cardiac disease mechanisms using induced pluripotent stem cell-derived cardiomyocytes: progress promises and challenges. Int J Mol Sci. 2020;21:4354.
16. Lian X, Hsiao C, Wilson G, Zhu K, Hazeltine LB, Azarin SM, Raval KK, Zhang J, Kamp TJ, Palecek SP. Robust cardiomyocyte differentiation from human pluripotent stem cells via temporal modulation of canonical Wnt signaling. Proc Natl Acad Sci USA. 2012;109:E1848-1857.
17. Zhao M, Tang Y, Zhou Y, Zhang J. Deciphering role of Wnt signalling in cardiac mesoderm and cardiomyocyte differentiation from human iPSCs: four-dimensional control of Wnt pathway for hiPSC-CMs differentiation. Sci Rep. 2019;9:19389.
18. Vidarsson H, Hyllner J, Sartipy P. Differentiation of human embryonic stem cells to cardiomyocytes for in vitro and in vivo applications. Stem Cell Rev Rep. 2010;6:108–20.
19. Kasahara A, Cipolat S, Chen Y, Dorn GW 2nd, Scorrano L. Mitochondrial fusion directs cardiomyocyte differentiation via calcineurin and Notch signaling. Science. 2013;342:734–7.
20. Fetterman KA, Blancard M, Lyra-Leite DM, Vanoye CG, Fonoudi H, Jouni M, DeKeyser JL, Lenny B, Sapkota Y, George AL Jr, Burridge PW. Independent compartmentalization of functional, metabolic, and transcriptional maturation of hiPSC-derived cardiomyocytes. Cell Rep. 2024;43: 114160.
21. Mummery CL, Zhang J, Ng ES, Elliott DA, Elefanty AG, Kamp TJ. Differentiation of human embryonic stem cells and induced pluripotent stem cells to cardiomyocytes: a methods overview. Circ Res. 2012;111:344–58.
22. Burridge PW, Matsa E, Shukla P, Lin ZC, Churko JM, Ebert AD, Lan F, Diecke S, Huber B, Mordwinkin NM, Plews JR, Abilez OJ, Cui B, Gold JD, Wu JC. Chemically defined generation of human cardiomyocytes. Nat Methods. 2014;11:855–60.
23. Jiang X, Lian X, Wei K, Zhang J, Yu K, Li H, Ma H, Cai Y, Pang L. Maturation of pluripotent stem cell-derived cardiomyocytes: limitations and challenges from metabolic aspects. Stem Cell Res Ther. 2024;15:354.
24. Lopaschuk GD, Jaswal JS. Energy metabolic phenotype of the cardiomyocyte during development, differentiation, and postnatal maturation. J Cardiovasc Pharmacol. 2010;56:130–40.
25. Garbern JC, Lee RT. Mitochondria and metabolic transitions in cardiomyocytes: lessons from development for stem cell-derived cardiomyocytes. Stem Cell Res Ther. 2021;12:177.
26. Chakrabarty RP, Chandel NS. Mitochondria as signaling organelles control mammalian stem cell fate. Cell Stem Cell. 2021;28:394–408.
27. Maroli G, Braun T. The long and winding road of cardiomyocyte maturation. Cardiovasc Res. 2021;117:712–26.
28. Parrotta EI, Scalise S, Scaramuzzino L, Cuda G. Stem cells: the game changers of human cardiac disease modelling and regenerative medicine. Int J Mol Sci. 2019;20:5760.
29. Julian LM, Stanford WL. Organelle cooperation in stem cell fate: lysosomes as emerging regulators of cell identity. Front Cell Dev Biol. 2020;8:591.
30. Simon HU. Autophagy in myocardial differentiation and cardiac development. Circ Res. 2012;110:524–5.
31. Xu Y, Zhang Y, Garcia-Canaveras JC, Guo L, Kan M, Yu S, Blair IA, Rabinowitz JD, Yang X. Chaperone-mediated autophagy regulates the pluripotency of embryonic stem cells. Science. 2020;369:397–403.
32. Li J, Maeji M, Balboula AZ, Aboelenain M, Fujii T, Moriyasu S, Bai H, Kawahara M, Takahashi M. Dynamic status of lysosomal cathepsin in bovine oocytes and preimplantation embryos. J Reprod Dev. 2020;66:9–17.
33. Duncan EM, Muratore-Schroeder TL, Cook RG, Garcia BA, Shabanowitz J, Hunt DF, Allis CD. Cathepsin L proteolytically processes histone H3 during mouse embryonic stem cell differentiation. Cell. 2008;135:284–94.
34. Park S, Huang H, Kwon W, Kim HY, Park JK, Han JE, Cho GJ, Han SH, Sung Y, Ryoo ZY, Kim MO, Choi SK. Cathepsin A regulates pluripotency, proliferation and differentiation in mouse embryonic stem cells. Cell Biochem Funct. 2021;39:67–76.
35. Jiang H, Cheng XW, Shi GP, Hu L, Inoue A, Yamamura Y, Wu H, Takeshita K, Li X, Huang Z, Song H, Asai M, Hao CN, Unno K, Koike T, Oshida Y, Okumura K, Murohara T, Kuzuya M. Cathepsin K-mediated Notch1 activation contributes to neovascularization in response to hypoxia. Nat Commun. 2014;5:3838.
36. Han Y, Feng H, Sun J, Liang X, Wang Z, Xing W, Dai Q, Yang Y, Han A, Wei Z, Bi Q, Ji H, Kang T, Zou W. Lkb1 deletion in periosteal mesenchymal progenitors induces osteogenic tumors through mTORC1 activation. J Clin Invest. 2019;129:1895–909.
37. Guo R, Hua Y, Rogers O, Brown TE, Ren J, Nair S. Cathepsin K knockout protects against cardiac dysfunction in diabetic mice. Sci Rep. 2017;7:8703.
38. Guo R, Hua Y, Ren J, Bornfeldt KE, Nair S. Correction: cardiomyocyte-specific disruption of cathepsin K protects against doxorubicin-induced cardiotoxicity. Cell Death Dis. 2019;10:933.
39. Guo R, Hua Y, Ren J, Bornfeldt KE, Nair S. Cardiomyocyte-specific disruption of cathepsin K protects against doxorubicin-induced cardiotoxicity. Cell Death Dis. 2018;9:692.
40. Yang H, Heyer J, Zhao H, Liang S, Guo R, Zhong L. The potential role of cathepsin K in non-small cell lung cancer. Molecules. 2020;25:4136.
41. Hua Y, Zhang Y, Dolence J, Shi GP, Ren J, Nair S. Cathepsin K knockout mitigates high-fat diet-induced cardiac hypertrophy and contractile dysfunction. Diabetes. 2013;62:498–509.
42. Lutgens E, Lutgens SP, Faber BC, Heeneman S, Gijbels MM, de Winther MP, Frederik P, van der Made I, Daugherty A, Sijbers AM, Fisher A, Long CJ, Saftig P, Black D, Daemen MJ, Cleutjens KB. Disruption of the cathepsin K gene reduces atherosclerosis progression and induces plaque fibrosis but accelerates macrophage foam cell formation. Circulation. 2006;113:98–107.
43. Vashum Y, Khashim Z. Obesity and cathepsin K: a complex pathophysiological relationship in breast cancer metastases, endocr metab immune disord drug. Targets. 2020;20:1227–31.
44. Funicello M, Novelli M, Ragni M, Vottari T, Cocuzza C, Soriano-Lopez J, Chiellini C, Boschi F, Marzola P, Masiello P, Saftig P, Santini F, St-Jacques R, Desmarais S, Morin N, Mancini J, Percival MD, Pinchera A, Maffei M. Cathepsin K null mice show reduced adiposity during the rapid accumulation of fat stores. PLoS ONE. 2007;2: e683.
45. Novinec M, Lenarcic B. Cathepsin K: a unique collagenolytic cysteine peptidase. Biol Chem. 2013;394:1163–79.
46. Lecaille F, Bromme D, Lalmanach G. Biochemical properties and regulation of cathepsin K activity. Biochimie. 2008;90:208–26.
47. Chen R, Dong H, Raval D, Maridas D, Baroi S, Chen K, Hu D, Berry SR, Baron R, Greenblatt MB, Gori F. Sfrp4 is required to maintain Ctsk-lineage periosteal stem cell niche function. Proc Natl Acad Sci USA. 2023;120: e2312677120.
48. Zhang W, Dong Z, Li D, Li B, Liu Y, Zheng X, Liu H, Zhou H, Hu K, Xue Y. Cathepsin K deficiency promotes alveolar bone regeneration by

promoting jaw bone marrow mesenchymal stem cells proliferation and differentiation via glycolysis pathway. Cell Prolif. 2021;54: e13058.
49. Dauth S, Schmidt MM, Rehders M, Dietz F, Kelm S, Dringen R, Brix K. Characterisation and metabolism of astroglia-rich primary cultures from cathepsin K-deficient mice. Biol Chem. 2012;393:959–70.
50. Yiangou L, Grandy RA, Osnato A, Ortmann D, Sinha S, Vallier L. Cell cycle regulators control mesoderm specification in human pluripotent stem cells. J Biol Chem. 2019;294:17903–14.
51. Kay M, Soltani BM, Aghdaei FH, Ansari H, Baharvand H. Hsa-miR-335 regulates cardiac mesoderm and progenitor cell differentiation. Stem Cell Res Ther. 2019;10:191.
52. Liu Y, Kaneda R, Leja TW, Subkhankulova T, Tolmachov O, Minchiotti G, Schwartz RJ, Barahona M, Schneider MD. Hhex and Cer1 mediate the Sox17 pathway for cardiac mesoderm formation in embryonic stem cells. Stem Cells. 2014;32:1515–26.
53. Tan X, Dai Q, Guo T, Xu J, Dai Q. Efficient generation of transgene- and feeder-free induced pluripotent stem cells from human dental mesenchymal stem cells and their chemically defined differentiation into cardiomyocytes. Biochem Biophys Res Commun. 2018;495:2490–7.
54. Fu H, Wang L, Wang J, Bennett BD, Li JL, Zhao B, Hu G. Dioxin and AHR impairs mesoderm gene expression and cardiac differentiation in human embryonic stem cells. Sci Total Environ. 2019;651:1038–46.
55. Kehat I, Kenyagin-Karsenti D, Snir M, Segev H, Amit M, Gepstein A, Livne E, Binah O, Itskovitz-Eldor J, Gepstein L. Human embryonic stem cells can differentiate into myocytes with structural and functional properties of cardiomyocytes. J Clin Investig. 2001;108:407–14.
56. Su L, Zhang G, Jiang L, Chi C, Bai B, Kang K. The role of c-Jun for beating cardiomycyte formation in prepared embryonic body. Stem Cell Res Ther. 2023;14:371.
57. Lian X, Bao X, Zilberter M, Westman M, Fisahn A, Hsiao C, Hazeltine LB, Dunn KK, Kamp TJ, Palecek SP. Chemically defined, albumin-free human cardiomyocyte generation. Nat Methods. 2015;12:595–6.
58. Lundy SD, Zhu WZ, Regnier M, Laflamme MA. Structural and functional maturation of cardiomyocytes derived from human pluripotent stem cells. Stem Cells Dev. 2013;22:1991–2002.
59. Fukushima H, Yoshioka M, Kawatou M, Lopez-Davila V, Takeda M, Kanda Y, Sekino Y, Yoshida Y, Yamashita JK. Specific induction and long-term maintenance of high purity ventricular cardiomyocytes from human induced pluripotent stem cells. PLoS ONE. 2020;15: e0241287.
60. Zhang JZ, Termglinchan V, Shao NY, Itzhaki I, Liu C, Ma N, Tian L, Wang VY, Chang ACY, Guo H, Kitani T, Wu H, Lam CK, Kodo K, Sayed N, Blau HM, Wu JC. A human iPSC double-reporter system enables purification of cardiac lineage subpopulations with distinct function and drug response profiles. Cell Stem Cell. 2019;24:802–11.
61. Meacham CE, DeVilbiss AW, Morrison SJ. Metabolic regulation of somatic stem cells in vivo. Nat Rev Mol Cell Biol. 2022;23:428–43.
62. Jahng JWS, Zhang M, Wu JC. The role of metabolism in directed differentiation versus trans-differentiation of cardiomyocytes. Semin Cell Dev Biol. 2022;122:56–65.
63. TeSlaa T, Chaikovsky AC, Lipchina I, Escobar SL, Hochedlinger K, Huang J, Graeber TG, Braas D, Teitell MA. Alpha-ketoglutarate accelerates the initial differentiation of primed human pluripotent stem cells. Cell Metab. 2016;24:485–93.
64. Hwang IY, Kwak S, Lee S, Kim H, Lee SE, Kim JH, Kim YA, Jeon YK, Chung DH, Jin X, Park S, Jang H, Cho EJ, Youn HD. Psat1-dependent fluctuations in alpha-ketoglutarate affect the timing of ESC differentiation. Cell Metab. 2016;24:494–501.
65. Li L, Chen K, Wang T, Wu Y, Xing G, Chen M, Hao Z, Zhang C, Zhang J, Ma B, Liu Z, Yuan H, Liu Z, Long Q, Zhou Y, Qi J, Zhao D, Gao M, Pei D, Nie J, Ye D, Pan G, Liu X. Glis1 facilitates induction of pluripotency via an epigenome-metabolome-epigenome signalling cascade. Nat Metab. 2020;2:882–92.
66. Chen X, Shen WB, Yang P, Dong D, Sun W, Yang P. High glucose inhibits neural stem cell differentiation through oxidative stress and endoplasmic reticulum stress. Stem Cells Dev. 2018;27:745–55.
67. Chen Y, Wu G, Li M, Hesse M, Ma Y, Chen W, Huang H, Liu Y, Xu W, Tang Y, Zheng H, Li C, Lin Z, Chen G, Liao W, Liao Y, Bin J, Chen Y. LDHA-mediated metabolic reprogramming promoted cardiomyocyte proliferation by alleviating ROS and inducing M2 macrophage polarization. Redox Biol. 2022;56: 102446.
68. Zhang W, Wang C, Hu X, Lian Y, Ding C, Ming L. Inhibition of LDHA suppresses cell proliferation and increases mitochondrial apoptosis via the JNK signaling pathway in cervical cancer cells. Oncol Rep. 2022;47:1–11.
69. Liu X, Zuo X, Sun X, Tian X, Teng Y. Hexokinase 2 promotes cell proliferation and tumor formation through the Wnt/beta-catenin pathway-mediated cyclin D1/c-myc upregulation in epithelial ovarian cancer. J Cancer. 2022;13:2559–69.
70. Thomas GE, Egan G, Garcia-Prat L, Botham A, Voisin V, Patel PS, Hoff FW, Chin J, Nachmias B, Kaufmann KB, Khan DH, Hurren R, Wang X, Gronda M, MacLean N, O'Brien C, Singh RP, Jones CL, Harding SM, Raught B, Arruda A, Minden MD, Bader GD, Hakem R, Kornblau S, Dick JE, Schimmer AD. The metabolic enzyme hexokinase 2 localizes to the nucleus in AML and normal haematopoietic stem and progenitor cells to maintain stemness. Nat Cell Biol. 2022;24:872–84.
71. Tang M, Dong X, Xiao L, Tan Z, Luo X, Yang L, Li W, Shi F, Li Y, Zhao L, Liu N, Du Q, Xie L, Hu J, Weng X, Fan J, Zhou J, Gao Q, Wu W, Zhang X, Liao W, Bode AM, Cao Y. CPT1A-mediated fatty acid oxidation promotes cell proliferation via nucleoside metabolism in nasopharyngeal carcinoma. Cell Death Dis. 2022;13:331.
72. Khacho M, Clark A, Svoboda DS, Azzi J, MacLaurin JG, Meghaizel C, Sesaki H, Lagace DC, Germain M, Harper ME, Park DS, Slack RS. Mitochondrial dynamics impacts stem cell identity and fate decisions by regulating a nuclear transcriptional program. Cell Stem Cell. 2016;19:232–47.
73. Yang X, Rodriguez ML, Leonard A, Sun L, Fischer KA, Wang Y, Ritterhoff J, Zhao L, Kolwicz SC Jr, Pabon L, Reinecke H, Sniadecki NJ, Tian R, Ruohola-Baker H, Xu H, Murry CE. Fatty acids enhance the maturation of cardiomyocytes derived from human pluripotent stem cells. Stem Cell Reports. 2019;13:657–68.
74. Yoshida S, Miyagawa S, Fukushima S, Kawamura T, Kashiyama N, Ohashi F, Toyofuku T, Toda K, Sawa Y. Maturation of human induced pluripotent stem cell-derived cardiomyocytes by soluble factors from human mesenchymal stem cells. Mol Ther. 2018;26:2681–95.
75. Turk V, Stoka V, Vasiljeva O, Renko M, Sun T, Turk B, Turk D. Cysteine cathepsins: from structure, function and regulation to new frontiers. Biochim Biophys Acta. 1824;2012:68–88.
76. Sun J, Sukhova GK, Zhang J, Chen H, Sjoberg S, Libby P, Xia M, Xiong N, Gelb BD, Shi GP. Cathepsin K deficiency reduces elastase perfusion-induced abdominal aortic aneurysms in mice. Arterioscler Thromb Vasc Biol. 2012;32:15–23.
77. Leeman DS, Hebestreit K, Ruetz T, Webb AE, McKay A, Pollina EA, Dulken BW, Zhao X, Yeo RW, Ho TT, Mahmoudi S. Lysosome activation clears aggregates and enhances quiescent neural stem cell activation during aging. Scienc. 2018;359:1277–83.
78. Liu P, Liu K, Gu H, Wang W, Gong J, Zhu Y, Zhao Q, Cao J, Han C, Gao F, Chen Q, Li W, Jiao J, Hu B, Zhou Q, Zhao T. High autophagic flux guards ESC identity through coordinating autophagy machinery gene program by FOXO1. Cell Death Differ. 2017;24:1672–80.
79. Yang HL, Lai ZZ, Shi JW, Zhou WJ, Mei J, Ye JF, Zhang T, Wang J, Zhao JY, Li DJ, Li MQ. A defective lysophosphatidic acid-autophagy axis increases miscarriage risk by restricting decidual macrophage residence. Autophagy. 2022;18:2459–80.

Publisher's Note